Activation of
NLRP3 inflammasome accelerates tau pathology

Inaugural-Dissertation

zur Erlangung des Doktorgrades

der Hohen Medizinischen Fakultät

der Rheinischen Friedrich-Wilhelms-Universität

Bonn

Shuangshuang Zhang

aus Jiangxi/China

2024

Angefertigt mit der Genehmigung
der Medizinischen Fakultät der Universität Bonn

1. Gutachter: Prof. Dr. Michael T. Heneka

2. Gutachter: Prof. Dr. Rayk Behrendt

Tag der Mündlichen Prüfung: 16.08.2023

Klinik für Neurodegenerative Erkrankungen & Gerontopsychiatrie (Universitätsklinikum Bonn)
Deutsches Zentrum für Neurodegenerative Erkrankungen
Direktor: Prof. Dr. Michael T. Heneka

Meinen Familien

Table of contents

List of abbreviations

Aβ	amyloid-β peptides
AD	Alzheimer's disease
ASC	apoptosis-associated speck- like protein containing a CARD
CaMKII	calmodulin-dependent protein kinase-II
CDK5	cyclin dependent protein kinase-5
CSF	cerebrospinal fluid
CNS	central nervous system
DAMP	danger-associated molecular pattern
GSK-3	glycogen synthase kinase-3
NFT	neurofibrillary tangles
NOD	nucleotide-binding oligomerization domain
NLR	NOD-like receptor
NLRP3	NACHT-, LRR- and pyrin domains-containing protein 3
PAMP	pathogen-associated molecular pattern
PHF	paired helical filaments
RT	room temperature
TLR	Toll-like receptor

1. Introduction

1.1 Alzheimer's disease

Alzheimer's disease (AD) is the most common cause of dementia, which affects an estimated of 5.8 million people age 65 or older in the US, and the number may grow up to 13.8 million by 2050 (Alzheimer's 2020). Characteristic symptoms among those who seek medical attention include progressive short-term memory failure, problems with orientation and difficulties with finding words (Heneka, Golenbock, and Latz 2015). In most cases, these symptoms are the prelude to AD. Most AD patients are diagnosed when they are at least 65 years old, but the pathological processes behind this devastating neurodegenerative disease may begin years before diagnosis (Jack et al. 2013) (Fig. 1). This suggests that aging mainly contributes to AD development.

Brains from AD patients show two types of lesions: 1) amyloid-β (Aβ) peptide deposits in extracellular space and 2) intracellular neurofibrillary tangles (NFTs) of hyperphosphorylated tau protein (Querfurth and LaFerla 2010) (Fig. 1). However, Aβ deposition and NFT aggregation may not explain all the clinical symptoms of AD: in recent years, neuroinflammation has been considered as a third hallmark of the disease (Heneka, Kummer, and Latz 2014).

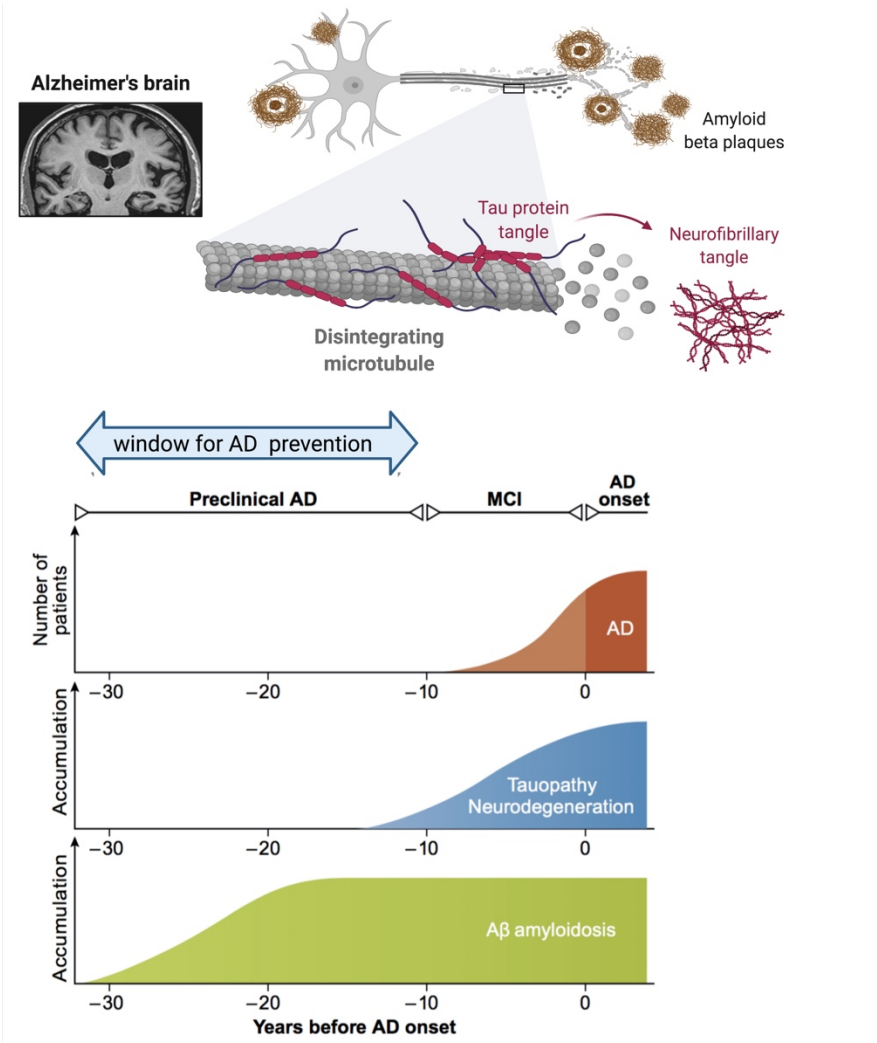

Fig. 1: Cortical pathology and neurological symptoms of AD. Deposits of amyloid-β (Aβ) and neurofibrillary tangles are the two types of lesions characteristic of AD. The disease appears to progress through three neurological phases: the *first* is the preclinical phase of AD without neurological symptoms, marked by Aβ accumulation in cortex; the *second* is mild cognitive impairment (MCI), marked by tau pathology and neurodegeneration without dementia; the *third* phase is AD, in which irreversible loss of neurons and neuronal circuits leads to dementia. Adapted from (Sasaguri et al. 2017).

1.2 Amyloid-β

According to the current paradigm, deposition of Aβ peptides is the first detectable stage of AD. Aβ is generated following sequential cleavage of the amyloid precursor protein by two aspartyl proteases: β-secretase 1 (also known as BACE1) and γ-secretase (Querfurth and LaFerla 2010). The major cleavage

products are Aβ40 and Aβ42, which can exist as monomers, oligomers, protofibrils and fibrils (Mattson 2004).

The active site of γ-secretase is formed by presenilin 1 and presenilin 2, which are encoded by the respective genes *PSEN1* and *PSEN2*. Certain mutations of *PSEN1* and *PSEN2* lead to excessive production of Aβ, which is responsible for most hereditary forms of AD (Bertram, Lill, and Tanzi 2010). In contrast, sporadic, non-hereditary cases of AD are at least partially attributed to decreased clearance of Aβ (Mawuenyega et al. 2010).

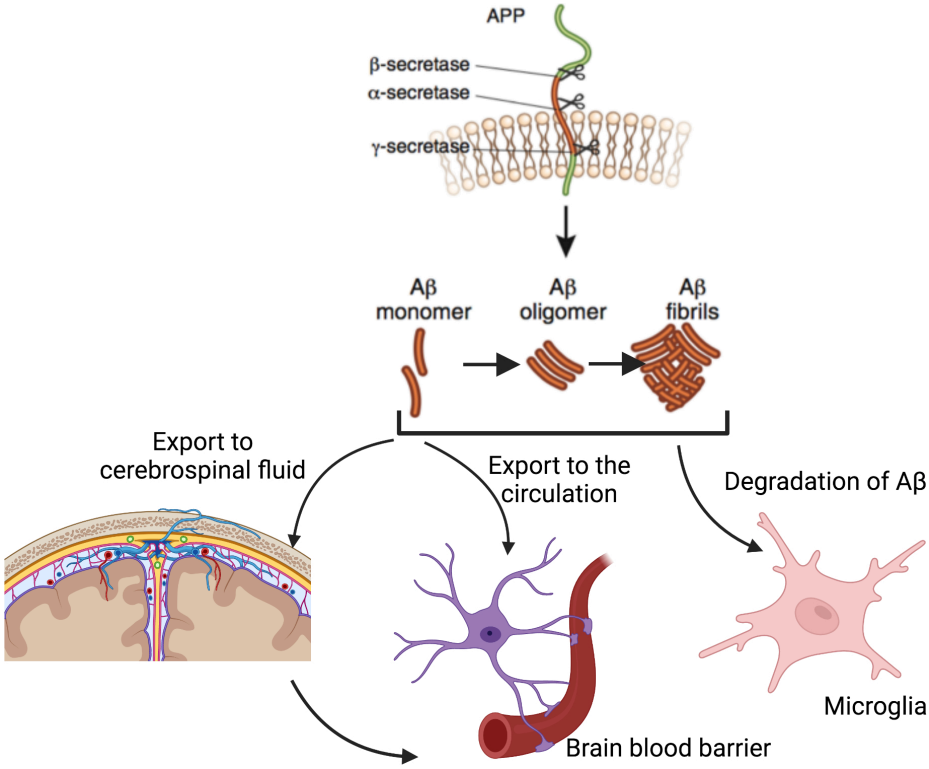

Fig. 2: Clearance of Aβ. The proteases α-, β-, and γ-secretase process amyloid precursor protein (APP) into Aβ. Monomers of Aβ can assemble into oligomers, and then into fibrils. Aβ can be exported into the extracellular fluid, and also into the circulation in a direct or indirect way. Microglia take up Aβ and degrade it, contributing to its clearance. Adapted from (Heneka, Golenbock, and Latz 2015).

Aβ is cleared from the brain through three mechanisms: 1) being exported into the cerebrospinal fluid (CSF); 2) being exported into the circulation; and 3) being locally degraded by microglia, cells which partially form the brain's innate immune system (Heneka, Golenbock, and Latz 2015) (Fig. 2). Approximately 50% of Aβ is

removed through the CSF and blood, and the remainder is taken up and degraded by microglia. These clearance pathways can compensate for one another to a certain extent: inhibiting one pathway can upregulate another. However, when the concentration of Aβ increases above a critical threshold, monomers oligomerize and deposit into Aβ fibrils, giving rise to senile plaques (Heneka 2017).

1.3 Tau pathology

Tau is a microtubule-associated protein expressed mainly in neurons. It stabilizes microtubules and promotes their assembly (Takemura et al. 1992). Various tau isoforms exist and differ in whether they contain four or three repeats (4R, 3R) and whether their amino-terminal domain contains no, one or two copies of a 29-residue sequence (0N, 1N, 2N).

During AD development, tau undergoes multiple post-transcriptional modifications, the most relevant of which is phosphorylation at multiple sites (Luna-Munoz et al. 2007; Noble et al. 2013). In AD and related disorders collectively referred to as "tauopathies", tau is hyperphosphorylated and accumulates intraneuronally presented as tangles of paired helical filaments (PHFs), straight filaments or twisted ribbons (Grundke-Iqbal et al. 1986). The degree of tau phosphorylation regulates its biological activity: hyperphosphorylation of tau inhibits its ability to promote microtubule assembly or even binding to microtubules at all (Alonso et al. 1994; Lindwall and Cole 1984).

Using monoclonal antibodies targeting tau proteins of different conformations, one group demonstrated that tau is conformationally altered in AD patients (Jicha, Berenfeld, and Davies 1999; Jicha et al. 1999) and in transgenic mice overexpressing human tau (Duff et al. 2000). Presumably this conformational alteration facilitates tau phosphorylation or impedes its dephosphorylation.

Together, the loss of soluble tau that would help stabilize microtubules and the accumulation of toxic intracellular aggregates may lead to neuronal death. This provides a reasonable explanation for the correlation between NFT burden and declined cognition in AD patients (Iba et al. 2013). Besides AD, tau pathology is also a characteristic in other neurodegenerative diseases (Table 1) (Iqbal et al. 2005), including frontotemporal dementia and parkinsonism linked to chromosome 17 (Goedert and Spillantini 2011).

Table 1 Neurodegenerative diseases characterized by abnormal hyperphosphorylation of tau ("tauopathies")

Primary Tauopathies
Frontotemporal dementia
Corticobasal degeneration
Progressive supranuclear palsy
Pick's disease
Argyrophilic grain disease
Chronic traumatic encephalopathy
Parkinsonism-Dementia complex of Guam
Secondary Tauopathies
Alzheimer's disease
Down syndrome

Adapted from (Iqbal et al. 2005).

1.4 Protein kinases, protein phosphatases and tau pathology

The mechanisms of tau aggregation are still not well understood, although tau hyperphosphorylation seems to be a prerequisite. This hyperphosphorylation may be caused by imbalances between kinases and phosphatases that target tau (Iqbal et al. 2005) (Fig. 3). Tau in AD is phosphorylated at more than 30 Ser/Thr residues (Hanger et al. 1998; Morishima-Kawashima et al. 1995), implying the activity of several protein kinases (Johnson and Hartigan 1999). Several of these

kinases have been identified (Iqbal et al. 2005), such as cyclin-dependent protein kinase-5 (CDK5), glycogen synthase kinase-3 (GSK-3), calcium- and calmodulin-dependent protein kinase-II (CaMKII) and stress-activated protein kinase p38.

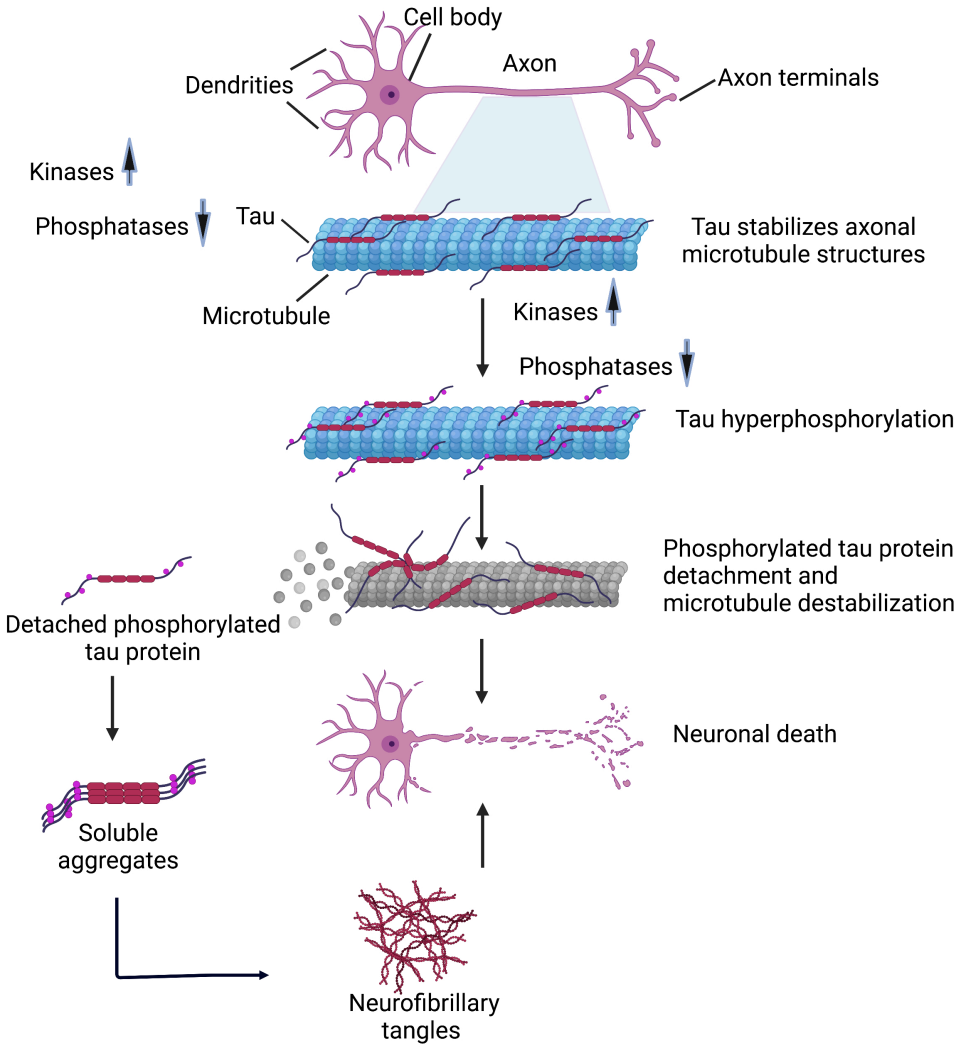

Fig. 3: Mechanism of neurofibrillary tangle formation and neuronal death. Unlike tau in healthy individuals, tau in AD is hyperphosphorylated and *N*-glycosylated. The *N*-glycosylation is thought to facilitate tau phosphorylation by kinases, while inhibiting tau dephosphorylation by phosphatases. Tau hyperphosphorylation destabilizes microtubules. In addition, the hyperphosphorylated tau aggregates into neurofibrillary tangles, which grow gradually and may eventually "choke" affected neurons to death.

GSK-3β and CDK5, both highly expressed in the brain (Lew et al. 1994; Woodgett 1990), have been associated with neurofibrillary pathology in all stages of PD (Pei et al. 1999; Pei et al. 1998). After phosphorylation by GSK-3β, tau inhibits

microtubule assembly (Utton et al. 1997). Inhibiting GSK-3β with lithium can reduce tau phosphorylation and its subsequent aggregation (Noble et al. 2005). CDK5 is regarded as a neuronal kinase whose activity requires interaction of the full-length subunits p35 with its proteolytic product, p25 (Kusakawa et al. 2000). Toxic insults such as Aβ and inflammation induce the cleavage of p35, which hyperactivates the enzyme (Cruz and Tsai 2004) and can lead to tau hyperphosphorylation.

The p38 kinase is a member of the family of mitogen-activated protein (MAP) kinases. Early in AD, p38 is activated and may be involved in tau phosphorylation within neurons (Pei et al. 2001).

CaMKII phosphorylates tau at Ser262, Ser356 and Ser416 (Singh et al. 1996; Yamamoto et al. 2005). Even the transient stimulation of CaMKII may lead to tau hyperphosphorylation (Iqbal et al. 2005).

While several kinases likely phosphorylate tau, few phosphatases have been identified that reduce the phosphorylation of hyperphosphorylated tau to normal levels. The best studied is phosphoseryl/phosphothreonyl protein phosphatase 2A (PP2A) (Liu et al. 2005). In fact, PP2A can regulate the activities of GSK3β, CDK5 (Louis et al. 2011) and CaMKII (Bennecib et al. 2001) to indirectly influence tau phosphorylation. Brains of AD patients show lower levels of PP2A and its activators, but higher levels of its inhibitors, than brains from age-matched controls (Sontag and Sontag 2014). One inhibitor is PP2A-specific methylesterase (PME-1), which removes a methyl group from the active site of PP2A, deactivating the enzyme (Xing et al. 2008).

1.5 Neuroinflammation and Alzheimer's disease

Aβ plays a pivotal role in AD pathogenesis (Walsh and Selkoe 2004), but whether Aβ plaques and NFTs cause AD remains uncertain. This uncertainty arises, in part, from the poor correlation between Aβ plaque burden and progression or severity of

dementia in AD (Gallardo and Holtzman 2019). For example, a transgenic mouse model of AD with widespread Aβ plaque deposition shows only slight cognitive deficits (Davis and Laroche 2003). NFTs seem to form later in the disease and may even occur, at least in some cases, downstream of Aβ deposition.

The current picture is that neuroinflammation is not a “bystander” in AD that is triggered by senile plaques and NFTs, but that neuroinflammation contributes to AD pathogenesis as much as, or even more than, plaques and NFTs do (Zhang et al. 2013). In fact, prolonged therapy with nonsteroidal anti-inflammatory drugs may reduce the risk of developing AD (in t' Veld et al. 2001; Sastre et al. 2003; Weggen et al. 2001). Several risk factors for AD are associated with inflammation (Fig. 4) (Heneka, Kummer, and Latz 2014), such as history of systemic inflammation, obesity and low physical activity (Iwashyna et al. 2010; Scarmeas et al. 2009; Whitmer et al. 2007). Consistent with AD as an inflammatory process, the brain and CSF of AD patients show elevated levels of chemokines, cytokines, complement factors and eicosanoids, which reflect inflammation-induced activation of innate and adaptive immune responses (Lue et al. 2001; Togo et al. 2002; Zotova et al. 2013). Over 20 gene polymorphisms have been demonstrated as risk factors in late-onset AD. Several of the genetic factors, such as *TREM2,* are involved in inflammation-induced innate immune responses (Guerreiro et al. 2013).

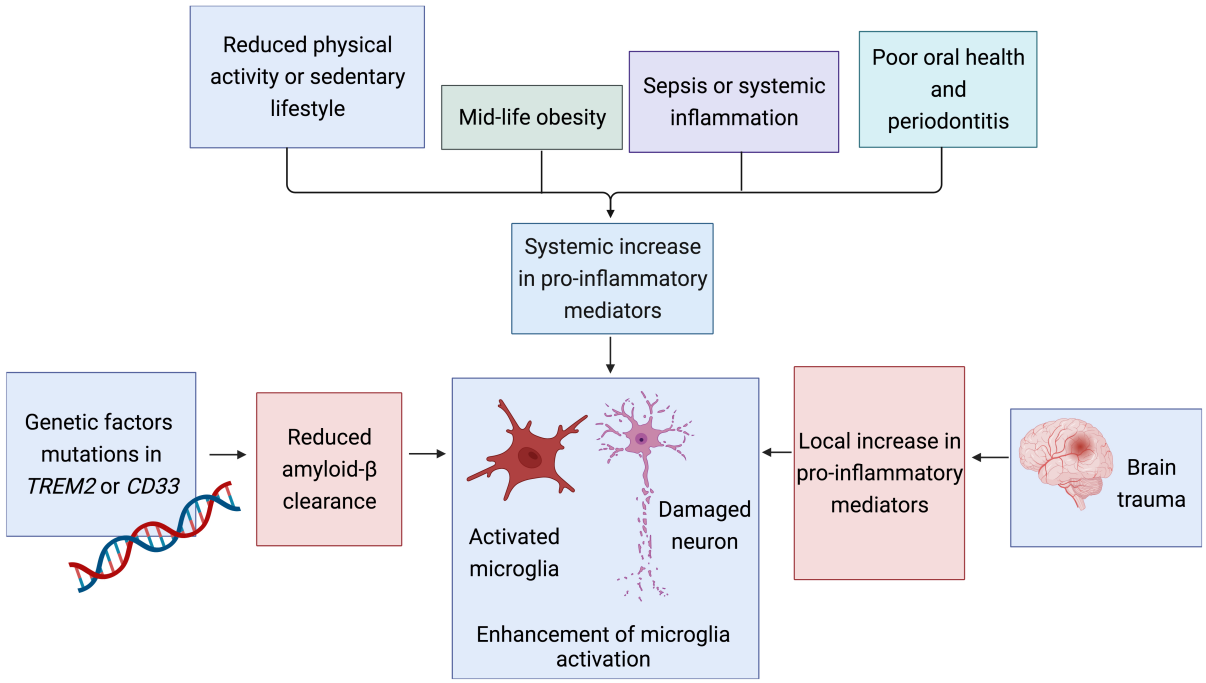

Fig. 4: Risk factors for AD enhance local or systemic inflammation, which activates innate immune responses. Adapted from (Heneka, Kummer, and Latz 2014).

1.6 Microglia

Microglia are resident phagocytes in the central nervous system. They are involved in the pathogenesis of many neurodegenerative and brain inflammatory diseases. After microglial populations are established, their numbers are maintained through a balance between proliferation and apoptosis (Askew et al. 2017), without replenishment from circulating progenitors (Ajami et al. 2007). The proportion of microglia varies from 5% to 12% in all glia cells throughout the rodent brain (Lawson et al. 1990) and 0.5%-16% in humans (Mittelbronn et al. 2001).

Traditionally, microglia have been classified into M1 and M2 phenotypes. M1 microglia show an activated, proinflammatory phenotype, while M2 microglia show a resting, non-inflammatory one. More recent work suggests that this binary scheme is oversimplified, with microglia in adults showing a more diverse set of phenotypes (Keren-Shaul et al. 2017; Ransohoff 2016). Microglia play a crucial role in maintaining brain homeostasis and neuronal plasticity (Heneka, Kummer,

and Latz 2014). They help determine and maintain neuronal connectivity by protecting and remodeling synapses, and they regulate neuronal growth and differentiation as well as formation of neural circuits (Kettenmann et al. 2011). Microglia are also the first line of immune defense against brain injury and inflammation (Ginhoux and Prinz 2015). They use their motile processes to search their surroundings for pathogens and cellular debris (Kettenmann et al. 2011).

To support their functions as immune cells, microglia express cytokines, various Toll-like receptors, pattern recognition receptors, and “NACHT-, LRR- and pyrin domains-containing protein 3” (NLRP3). The pattern recognition receptors bind to so-called danger-associated molecular patterns, which include misfolded proteins, aggregated peptides (Heneka, Kummer, and Latz 2014); this binding initiates an immune response in microglia (Heneka 2017). Pattern recognition receptors also sense oligomeric Aβ and aggregated fibrillar Aβ (Halle et al. 2008) as well as NFTs (Morales et al. 2013). Indeed, activated microglia co-localize with Aβ plaques and tau oligomers in brain tissues of both AD patients and transgenic mouse models (Nicoll et al. 2003; Nilson et al. 2017; Radde et al. 2006; Zotova et al. 2013). Fibrillar Aβ-induced activation of microglia results in the release of proinflammatory cytokines, e.g. IL-1β, IL-6 and TNF-α, and also the upregulation of integrin markers CD11b, CD11c and CD68 (Jana, Palencia, and Pahan 2008).

Activated microglia can exert beneficial or harmful effects depending on the pathophysiological context. When microglia react to pathogen- or danger-associated molecular patterns, they can respond acutely to resolve the problem rapidly. In contrast, their continuous response to ongoing accumulation of Aβ, neuronal debris and pro-inflammatory signaling factors in AD can lead to pathological chronic neuroinflammation, exacerbating the underlying disease (Heneka et al. 2015).

1.7 NLRP3 inflammasome

The most well characterized inflammasomes include NLRP1, NLRP3, and NLRC4. NLRP3 is a NOD-like receptor, which is part of a family of intracellular pattern recognition receptors. NOD-like receptors contain three domains: the nucleotide-binding oligomerization (NACHT) domain, the C-terminal leucine-rich repeat (LRR) domain, and the N-terminal effector domain. The N-terminal effector domain can be: 1) a pyrin domain (PYD), which is a protein-protein interaction domain; 2) a recruitment domain (CARD); 3) a baculovirus inhibitor of apoptosis repeat domain (BIR) (Martinon and Tschopp 2005; Latz 2010) (Fig. 5).

Ribonucleotides can bind to NACHT domains and thereby regulate self-oligomerization and activation of NOD-like receptors (Duncan et al. 2007). LRR domains interact with pathogen-associated molecular patterns (Stutz, Golenbock, and Latz 2009) and damage-associated patterns (Venegas and Heneka 2017). N-terminal effector domains mediate specific protein-protein interactions, and they serve as the basis for classifying NOD-like receptors (Latz 2010).

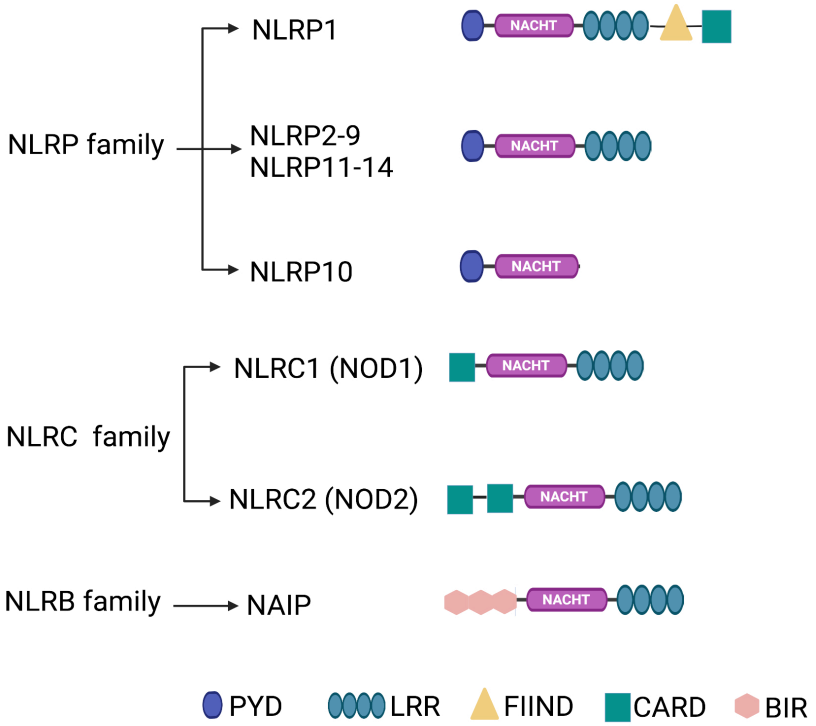

Fig. 5: Classification of NOD-like receptors (NLRs) based on constituent domains. NLRs contain three domains: the N-terminal effector domain, the nucleotide-binding oligomerization (NACHT) domain, and the C-terminal leucine-rich repeat (LRR) domain. BIR, baculovirus inhibitor of apopotosis repeat domain; CARD, caspase activation and recruitment domain; FIIND, function-to-find domain; PYD, pyrin domain. Adapted from (Venegas and Heneka 2019).

Upon activation, NLRP3 complexes with pro-caspase 1 and “apoptosis-associated speck-like protein” (ASC), which contains a C-terminal CARD domain. This complex, referred to as the activated NLRP3 inflammasome induces the secretion of IL-1β and IL-18 (Walsh, Muruve, and Power 2014). This complex appears to contribute to AD (Guo, Callaway, and Ting 2015; Heneka 2017; Heneka, Kummer, and Latz 2014), in part by upregulating levels of proinflammatory cytokines such as IL-18, IL-1β and cleaved caspase-1 in brain tissue of patients with early-onset disease (Heneka et al. 2013). NLRP3 can sense pathogen- and damage-associated molecular patterns as well as Aβ aggregates (Dostert et al. 2008; Mariathasan et al. 2006; Martinon et al. 2006). Deficiency of any of the components of the activated NLRP3 inflammasome protects APP/PS1 mice from amyloid pathology (Heneka et al. 2013). Conversely, treating mice with lipopolysaccharide (LPS) creates systemic inflammation that activates the NLRP3 inflammasome and prevents microglia from clearing Aβ (Tejera et al. 2019). The role of NLRP3 in driving AD is supported by genome-wide association studies in which AD risk was influenced by polymorphisms in genes encoding proteins that assist receptors for IL-1α, IL-1β and IL-1 (McGeer and McGeer 2001; Ramanan et al. 2015).

NLRP3 inflammasomes are activated in two steps (Fig. 6) (Heneka, McManus, and Latz 2018). First, binding of a pathogen-associated molecular pattern such as LPS to TLR4 “primes” microglia, leading nuclear factor-κB (NFκB) and other transcription factors to induce expression of pro-IL-1β. Second, a damage-associated molecular pattern such as ATP or Aβ “activates” microglia to pump K+

out of microglia, leading to activation of the NLRP3 inflammasome. Cleaved-caspase-1 furtherly cleaves IL-1β and IL-18 into corresponding active forms.

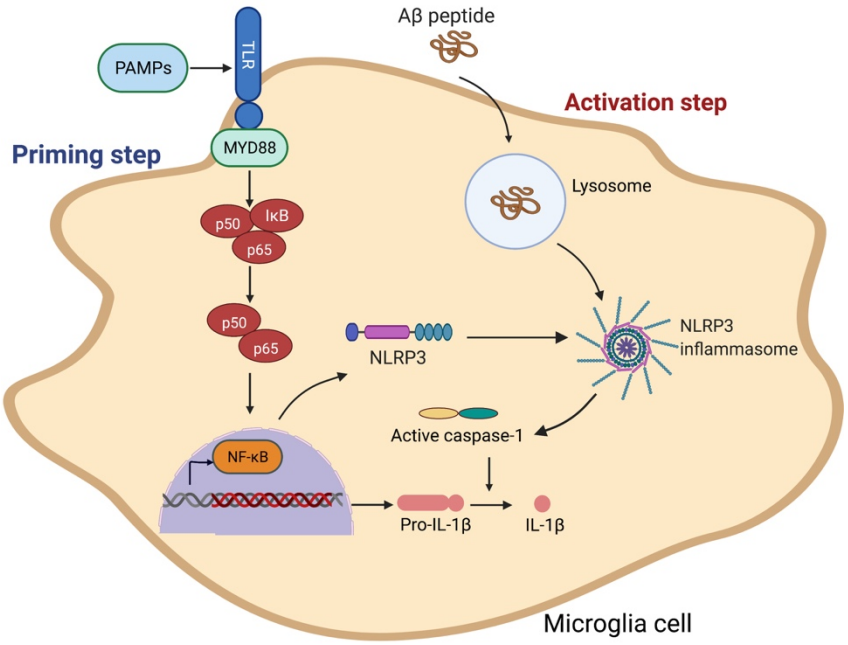

Fig. 6: Activation of the NLRP3 inflammasome in microglia. Activation of the inflammasome, which is tightly controlled, requires a priming step and an activation step. In the priming step, binding of pathogen-associated molecular patterns (PAMPs) to TLR4 (Toll-like receptor 4) causes a pathway involving the myeloid differentiation primary response protein (MYD88) and nuclear factor-κB (NF-κB) to induce expression of pro-IL-1β. In the activation step, DAMPs such as Aβ damage lysosomes, which induces assembly of the NLRP3 inflammasome. Activated caspase-1 cleaves pro-IL-1β into IL-1β, inducing the release of proinflammatory cytokines. Adapted from (Heneka, McManus, and Latz 2018).

1.8 ASC specks

Under normal conditions, the ASC protein is located in the cytoplasm and nucleus (Masumoto et al. 1999), but it oligomerizes into long filamentous structures called “ASC specks” when local conditions activate the NLRP3 inflammasome. ASC specks can grow to a diameter of 1 µm and therefore become detectable. Intracellularly only one ASC speck forms after inflammasome activation in most cells. Thus, analysis of the proportion of microglia containing ASC specks is often used as an upstream indicator of NLRP3 activation (Heneka 2017; Stutz et al. 2013).

ASC specks have been detected inside and outside of microglia in brains of AD patients and APP/PS1 mice brains. These specks show a prion-like ability to amplify neuroinflammatory responses (Fig. 7) (Venegas and Heneka 2019): they leave microglia and enter the extracellular space via pyroptosis, then other microglia or innate immune cells can internalize them (Baroja-Mazo et al. 2014). When microglia take up ASC specks, their NLRP3 inflammasomes become activated; in this way, ASC specks propagate the activation of inflammation between microglia (Broderick and Hoffman 2014; Franklin et al. 2014).

Once ASC specks are released into the extracellular space, they can rapidly bind to Aβ and accelerate its aggregation (Venegas et al. 2017). In that study, deficiency of ASC in APP/PS1 mice led to smaller cerebral Aβ load and milder spatial memory deficit. These findings suggest that ASC is directly involved in Aβ deposition early during Aβ accumulation.

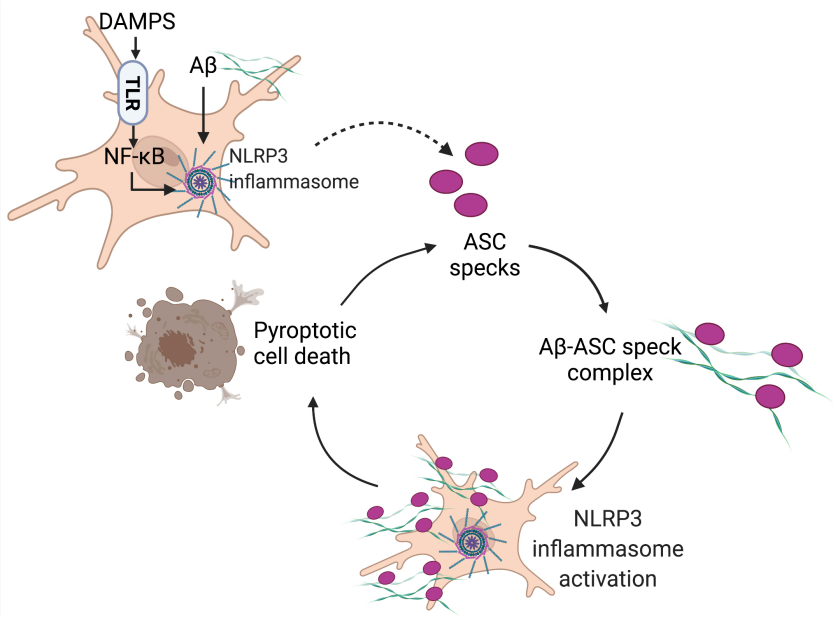

Fig. 7: Prion-like effect of ASC specks. Binding of damage-associated molecular patterns (DAMPs) to TLR on microglia triggers the release of ASC specks into the extracellular space, where they are internalized by surrounding microglia. Inside microglia, the specks induce NLRP3 inflammasome activation. At the same time, extracellular ASC specks can bind to amyloid-β (Aβ) and promote their aggregation. Both of these processes sustain neuroinflammation in AD. Adapted from (Venegas and Heneka 2019) and (Friker et al. 2020).

1.9 Aim of the work in this thesis

Extensive studies *in vitro* and *in vivo* indicate an important role of NLRP3 inflammasome activation in Aβ pathology in AD. In contrast, whether inflammasome activation also contributes to tau pathology in AD is unclear. The work described in this thesis aimed to explore this question and the underlying molecular mechanisms.

2. Materials and Methods

2.1 Materials

2.1.1 General materials

Product	Catalog or product no.	Company
Pipette tip, 10 µl	70.1130.600	Sarstedt
Pipette tip, 200 µl	70.760.502	Sarstedt
Pipette tip, 1000 µl	70.762.100	Sarstedt
Laboratory marker, black	PRCI1400-20-PDC	VWR International
Test tube, 50 ml	227261	Greiner Bio-One GmbH
Test tube, 15 ml	188271	Greiner Bio-One GmbH
Test tube, 5 ml	55,1579	Sarstedt
96-well microplates	655101	Greiner Bio-One GmbH
Needle, 27 gauge, 1/2-inch	300635	Becton Dickinson Medical
Disposable syringes, 1 ml	10303002	B Braun
Safe-lock reaction vessels, 1.5 ml	5409331	Eppendorf
Safe-lock reaction vessels, 2 ml	5409341	Eppendorf
Parafilm roll	P7793-1EA	Sigma-Aldrich
Aluminum foil, 30 cm x 10 m	3460511	Lyreco
Filter tip, 2.5 µl	701114215	Sarstedt
Filter tip, 20 µl	701130217	Sarstedt
Filter tip, 200 µl	70760216	Sarstedt

Filter tip, 1000 µl	70762216	Sarstedt
Gloves, small	5437673	Omnilab
PCR tubes, 0.2 ml, 8-strip	211-3264	VWR International

2.1.2 Chemicals

Product	**Catalog or product no.**	**Company**
Agarose	35-1020	VWR International
Amyloid β-Protein (1-42)	H-7442.1000	Bachem
Bis-Tris for buffer solutions	A1025	AppliChem
COMPLETE	11697498001	Sigma
D(+)-saccharose	4621,1	Carl Roth
EGTA	3054,1	Carl Roth
Acetic acid	3738,1	Carl Roth
Formaldehyde, 16%	18814-20	Polysciences
Glycin	3790,2	Carl Roth
Pepsin from porcine gastric mucosa	P7000	Sigma-Aldrich
Protease/phosphatase inhibitor cocktail (100X)	5872S	New England Biolabs
RedSafe	21141	INtRON Bio
Thioflavine S, practical grade	T1892	Sigma-Aldrich
Tris base	5429,3	Carl Roth
Triton X 100	3051,3	Carl Roth
Xylene, S	158692	MP Biomedicals
Orange G		Bernd Kraft
Phenylmethylsulfonylfluoride (PMSF)	6367,1	Roth
Sodium azide	26628-22-8	Sigma-Aldrich
Ethanol, 99,5%	——	DZNE Lab Management

EconoTaq PLUS GREEN Mastermix	30033-1-LU	BioCat
ELISA Substrate Solution	34029	Thermo Fisher

2.1.3 Cell culture supplies

Product	**Catalog or product no.**	**Company**
Adenosine triphosphate (ATP)	tlrl-atp	InvivoGen
Lipopolysaccharide (LPS)	tlrl-eklps	InvivoGen
B-27 supplement	17504044	LIFE Technologies
DMEM with GlutaMAX	10565018	LIFE Technologies
Fetal bovine serum	10270106	LIFE Technologies
1x Hanks' balanced salt solution (HBSS)	24020091	LIFE Technologies
Trypsin (2.5%)	15090046	LIFE Technologies
DNase	DN25-100MG	Sigma-Aldrich
Poly-L-lysine (PLL)	P1524-100MG	Sigma-Aldrich
Dulbecco's phosphate-buffered saline (DPBS)	14190169	Thermo Fisher
HBSS (10X), phenol red	14180046	Thermo Fisher
N-2 supplement (100X)	17502048	Thermo Fisher
Neurobasal medium	21103049	Thermo Fisher
Penicillin-streptomycin	15070063	Thermo Fisher
Trypsin-EDTA (0.25%) with phenol red	25200056	Thermo Fisher
IL-1β receptor antagonist, 100 nM	AF771-SP	R&D Systems
IRAK4 inhibitor, 20 μM	PF06650833	Sigma-Aldrich
MEK inhibitor (UO126), 10 μM	9903	Cell Signaling

2.1.4 Kits

Product	Catalog or product no.	Company
BCA assay kit	23225	Thermo Scientific
Mouse IL-1β ELISA kit	DY401	R&D Systems
ABC Elite kit	PK-6100	VectorLab
DAB peroxidase (HRP) substrate kit (with nickel)	SK-4100	VectorLab

2.1.5 Western blot supplies

Product	Catalog or product no.	Company
NuPAGE LDS Sample Buffer (4X), 10 mL	NP0007	Thermo Scientific
PageRuler Prestained Protein Ladder, 8 x 250 µL	26616X4	Thermo Scientific
4-12% Bis-Tris Protein Gels, 15-well	NP0336BOX	Invitrogen
4-12% Bis-Tris Protein Gels, 20-well	WG1402BOX	Invitrogen

2.1.6 DAB staining reagents

Product	Catalog or product no.	Company
3,3'-diaminobenzidine tetrahydrochloride	D5905	Sigma-Aldrich
ProLong Gold Antifade Mounting Medium with DAPI	DY401	R&D Systems
Cytoseal 60 (mounting medium)	8310-4	Thermo Fisher

2.1.7 Primary antibodies

Antigen recognized	Catalog no.	Application, Dilution	Provider
pTau-S416	ab119391	IF, 1:1000	Abcam
Tau5	MA5– 12808	WB, 1:500	Thermo Fisher Scientific
MC1	----	WB, 1:1000	gift from P. Davies
PHF-1	----	WB, 1:1000	gift from P. Davies
AT8-biotinylated	MN1020B	IF, 1:500	Thermo Fisher Scientific
β-actin	4967	WB, 1:2000	Cell Signaling
pCaMKIIα	12716T	WB, 1:1000	Cell Signaling
CaMKIIα	50049S	WB, 1:1000	Cell Signaling
pGSK-3β	612313	WB, 1:1000	BD
GSK-3β	9315S	WB, 1:1000	Cell Signaling
p25/p35	2680S	WB, 1:1000	Cell Signaling
demPP2A	05–577	WB, 1:500	Merck Millipore
PP2A subunit C	2259T	WB, 1:1000	Cell Signaling
PME-1	07–095	WB, 1:1000	Merck Millipore

dem, demethylated; IF, immunofluorescence; p, phosphorylated; WB, western blotting

2.1.8 Secondary antibodies

Product	Species recognized	Application, Dilution	Company
IRDye 680RD	Rabbit	WB, 1:10000	LI-COR Biosciences
IRDye 680RD	Mouse	WB, 1:10000	LI-COR Biosciences
IRDye 800CW	Rabbit	WB, 1:20000	LI-COR Biosciences
IRDye 800CW	Mouse	WB, 1:20000	LI-COR Biosciences
Alexa Fluor-555	Rabbit	IF, 1:500	Invitrogen

IF, immunofluorescence; WB, western blotting

2.1.9 Instruments

Instrument	Catalog or product no.	Company
Centrifuge	5424	Eppendorf
Centrifuge	5424R	Eppendorf
Centrifuge	Megafuge 40R	Thermo Scientific
Stereomicroscopy	SMZ-168 Series	Motic
Rotor	TLA120.1	Beckman Coulter
Rotor	FA-45-24-11 5425	Eppendorf
Rotor	FA-45-24-11 5425 R	Eppendorf
Heat block	ThermoMixer C	Eppendorf
Vibratome	G560E	Scientific Industries
Gel electrophoresis power supply	EV3020	Consort
Weighing balance	Explorer EX224	Ohaus
Western blotting chamber	WR0100	Invitrogen
-80℃ Freezer	V86G-500.1	EWALD Innovationstechnik
Precellys tissue homogenizer	P000669-PR240-A	Bertin Instruments
Plate Reader Infinite 200 PRO	——	Tecan
Imaging System Odyssey CLx	——	Licor
AxioScan.Z1 slide scanner	——	Zeiss
ChemiDoc XRS gel imaging system	——	BioRad

2.1.10 Software

Product	Version	Company
Prism for Mac OS X	7.0e	Dotmatics
ImageJ/FiJi software	2.0.0.-rc-67/1.52c	Advansta
ImageStudio	5.2.5	LI-COR
Adobe Photoshop CS5	12.0.1	Adobe

2.2 Methods

2.2.1 Animals

Animals for experiments were maintained and handled according to the local government regulations. All animal protocols were approved by the local ethical committee (LANUV NRW 84–02.04.2017.A226 and 81-02.04.2021.A221). Mice were housed under standardized conditions at 22 °C on a 12-h light/dark cycle with free access to food and water in the animal facility at the University Hospital of Bonn.

Experiments in this work involved C57BL/6 mice heterozygous for the THY-Tau22 transgene (hereafter “Tau22 mice”), which expresses a four-repeat isoform of human tau (1N4R) containing the mutations P301S and G272V under the control of the Thy1.2 promoter (Schindowski et al. 2006). Both male and female mice were used in experiments, since the two sexes do not differ significantly in tau pathology (Schindowski et al. 2006).

Some experiments were carried out with transgenic mice lacking the gene encoding ASC ($Asc^{-/-}$) or NLRP3 ($Nlrp3^{-/-}$). These mice have been described previously (Kanneganti et al. 2006) and were purchased from Millennium Pharmaceuticals (Cambridge, MA, USA). Some experiments were carried out using crosses between Tau22 mice and $Asc^{-/-}$ or $Nlrp3^{-/-}$ mice, referred to as Tau22/$Asc^{-/-}$ or Tau22/$Nlrp3^{-/-}$. Mice of both sexes were assigned randomly to

different groups. Mice were used at 11 months of age, or at 5 months after stereotaxic surgery (see section 2.2.2).

2.2.2 Mouse tissue isolation

At the end of experiments, mice were anesthetized by injecting ketamine (100 mg/kg) and xylazine (10 mg/kg) intraperitoneally, and then perfused with ice-cold phosphate-buffered saline (PBS) transcardially. Brains were taken out and hemispheres were either separated or not. Brain samples to be analyzed by immunohistochemistry were fixed at 4 °C in 4% paraformaldehyde (PFA) in PBS for 24 h (if one hemisphere) or 48 h (if full brain). Samples were washed with PBS and stored in PBS containing sodium azide at 4 °C until they were sectioned to a thickness of 40 µm on a Leica Vibratome. When only one hemisphere was fixed in PFA, the other was dissected into cortex and hippocampus on ice, frozen on dry ice and later stored at −80 °C. Perfusion and dissection were performed by Dr. Christina Ising, Dr. Carmen Venegas and Stephanie Schwartz (University of Bonn Hospital, Bonn, Germany). Tissues were sectioned by Ana Vieira-Saecker (University of Bonn Hospital, Bonn, Germany).

2.2.3 Stereotaxic surgery

For intracerebral injections, 3-month-old mice were anesthetized with ketamine (100 mg/kg) and xylazine (10 mg/kg), eye ointment was applied to prevent the eyes from drying out, and the animals were placed on a heating pad and fixed in a stereotaxic frame (Narishige, London, UK). Hair around the intended incision site was removed, the skin was sterilized, and a small incision was made. The periosteum was removed manually using a cotton swab, and the sutures were visualized by applying a small amount of 30% hydrogen peroxide. Using a Dremel device, a small hole was drilled into the skull at the following coordinates: anteroposterior -2.5 mm, mediolateral ± 2 mm, dorsoventral -1.8 mm. ASC specks were prepared as described previously (Venegas et al. 2017). One hippocampus was injected with vehicle, and the other was injected with ASC specks in vehicle. Injections were performed using a Hamilton syringe attached to an automatic

injector in the stereotaxic frame. The injection speed was controlled at 0.5 µl/min, and the total injection volume was 2 µl. The needle was left in place for 10 min before withdrawal, then the wound was closed by suturing. For three days after the procedure, mice received subcutaneous injections of analgesics (Carprofen). Injections and surgeries were performed by Dr. Carmen Venegas (University of Bonn Hospital, Bonn, Germany).

2.2.4 Primary microglial culture and activation of microglia *in vitro*

Primary murine microglia cell cultures were prepared from pups of C57BL/6 mice (hereafter referred to as wild-type), $Asc^{-/-}$ mice or $Nlrp3^{-/-}$ mice. Brains were isolated from newborn mice (P0-P3) and placed in precooled Hank's buffered saline solution (HBSS). Meninges were removed under a stereomicroscope, and cerebellum as well as both hemispheres were washed three times with HBSS. Tissues were then incubated in 0.25% trypsin at 37 °C for 5 min, 200 µl of 5 mg/ml DNase was added, and the mixture was pipetted carefully up and down within a 1-ml tip attached to a 5-ml pipettor.

To halt trypsin digestion, DMEM with 10% FCS and 100 U/ml penicillin/streptomycin was added. The suspension was collected and centrifuged at 300 g for 5 min at 4 °C, then the pellet was re-suspended in DMEM with 10% FCS seeded into precoated flasks. Before seeding, the flasks had been coated with 0.1% poly-D-lysine (PLL), then washed three times with Dulbecco's phosphate-buffered saline (DPBS).

After 24 h of incubation, two-thirds of the culture medium was replaced with fresh DMEM containing 10% FCS and 10% L929. At 7-10 days later, microglia were harvested from the mixed cultures by shaking; they were counted in a Neubauer chamber and plated in DMEM supplemented with 1% N-2 supplement.

In some experiments, neurons were treated with microglia-conditioned medium. In this case, mixed glial cultures were incubated in Neurobasal supplemented with

100 U/ml penicillin/streptomycin and 2% B-27 for at least 12 h before applying treatments, then microglia were isolated by up to three rounds of shaking.

Microglia were plated at 2 x 10^6 cells per well in a 6-well plate in DMEM containing 10% FCS on the morning of day 0. The medium was changed to the required medium on the evening of day 1, then the experiment was performed on day 2. Microglia were primed with 100 ng/ml ultrapure LPS for 3.5 h, washed once with warm DPBS, then treated with 10 mM ATP for 30 min. The conditioned medium was collected and centrifuged at 300 g for 5 min at 4 °C. The supernatant was transferred to a new tube and stored at -80 °C. Levels of secreted IL-1β were measured by enzyme-linked immunosorbent assay (ELISA) (see section 2.2.7).

2.2.5 Primary neuronal cultures

Primary mouse neuronal cultures were generated from newborn wild-type and Tau22 pups (P0). Hippocampi were dissected out after meninges were removed from brains. Samples from Tau22 pups were kept on ice while genotyping was performed on tail samples. Hippocampal tissue from mice with the same genotype was pooled, washed twice in HBSS, incubated for 10-15 min at 37 °C with 0.15% trypsin and 0.2 µg/ml DNase, washed three times with HBSS, then triturated carefully to generate a single-cell suspension. The suspension was centrifuged at 300 g for 5 min at 4 °C and resuspended in Neurobasal medium. Cells were counted and 70,000 cells/well were plated onto PLL-coated 24-well plates in Neurobasal medium containing B-27. Cells were used in experiments after 12-18 days in culture. Neuronal cultures were generated by Sabine Optiz (University of Bonn Hospital, Bonn, Germany).

2.2.6 PCR genotyping from animal tail

Tail samples from Tau22 pups were lysed in 75 µl lysis buffer (25 mM NaOH, 0.2 mM EDTA, pH 12.0) at 95 °C for 45-60 min. The samples were centrifuged for 1-2 min at 37 °C, then 75 µl neutralization buffer (4 µM Tris-HCl, pH 5.0) was added and mixed, and samples were stored at -20 °C.

To confirm the appropriate transgene, genotyping PCR was performed using the following primers: Tau 23, 5'-TCACCCGTGGTCTGTCTTGGC-3'; Tau25, 5'-CATATGCCACCCACCCGGGAG-3'; internal control primer CO4, 5'-CTAGGCCACAGAATTGAAAGATCT-3' and internal control primer CO5, 5'-GTAGGTGGAAATTCTAGCATCATCC-3'. Each PCR reaction (20 µl) contained 1x EconoTaq PLUS GREEN Mastermix, 10 µM of each primer and 1 µl DNA. A reaction with water instead of template DNA served as the negative control. The expected amplification products were 600 bp for the tau transgene and 324 bp for the internal control.

Samples were incubated in a PCR cycler at 95 °C for 2 min, followed by 30 cycles of denaturation at 95 °C for 30 sec, primer annealing at 62 °C for 30 sec, extension at 72 °C for 45 sec and a final extension time of 5 min at 72 °C. An aliquot of sample (10 µl) was loaded onto a 2% agarose gel (Peqlab agarose dissolved in 1x TAE by heating, supplemented with 5% RedSafe), in parallel with 1-kb DNA ladder (5 µl) as reference. Gels were imaged using the ChemiDoc XRS gel imaging system.

2.2.7 ELISA-based quantification of IL-1β

The level of IL-1β was quantified using a commercial ELISA kit according to the manufacturer's instructions and the reagents in Table 2.

Table 2 ELISA reagents and preparation of working solutions

Reagent	**Final dilution/composition of working solution**	**Diluent to obtain working solution**
Wash buffer	1 x PBS, 0.05% Tween-20	Deionized water
Stop solution	1 M 2 N H_2SO_4	Deionized water
Coating buffer	1 x PBS	Deionized water
Capture antibody	1:250	Coating buffer

Reagent diluent	1% bovine serum albumin	1 x PBS
Standard for calibration	See below	Reagent diluent
Detection antibody	1:250	Reagent diluent
Streptavidin-HRP	1:40	Reagent diluent

To prepare standards for a calibration curve, each vial was reconstituted in 500 µl of reagent diluent, and 2-fold serial dilutions were prepared using the same diluent in order to generate a seven-point calibration curve (Fig. 8).

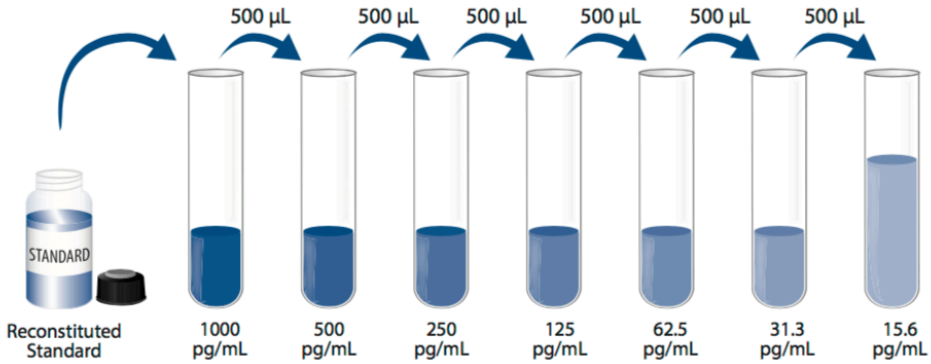

Fig. 8: Preparation of standards for building a calibration curve to determine levels of IL-1β secreted by primary mouse microglia. For each tube, original solution was diluted 1:2 with reagent diluent (see Table 2).

A 96-well ELISA plate was coated with 100 µl/well of capture antibody in coating buffer. The plate was sealed and incubated overnight at 4 °C, washed three times with more than 250 µl/well wash buffer, blotted dry on absorbent paper to remove residual buffer, blocked with 200 µl of manufacturer-supplied diluent, and incubated at room temperature (RT) for 1 h. The plate was aspirated, washed three times with wash buffer, then blotted dry on absorbent paper. Standard and experimental samples were added to the appropriate wells (100 µl/well). The plate was sealed, incubated at RT for 2 h, washed three times with wash buffer, and blotted dry on absorbent paper. Diluted detection antibody (100 µl/well) was added to the appropriate wells, then the plate was sealed, incubated at RT for 1 h, and

washed three times with wash buffer. Diluted horseradish peroxidase-conjugated streptavidin (100 µl/well) was added, and the plate was sealed, incubated at RT for 30 min, and washed three times with wash buffer. 1 x TMB Solution (100 µl/well) was added, plates were incubated for less than 15 min, then stop solution (100 µl/well) was added to halt the color change while it still was within its linear response range. Absorbance was measured at 450 nm using a Tecan plate reader.

2.2.8 Treatment of neurons with conditioned medium from microglia

Primary neurons were plated at 70,000 cells per well in a 24-well plate and cultured for 12-18 days. Then conditioned medium was collected from all neuronal cultures, pooled into a single tube, and spun at 300 g for 1 min at RT. 300 µl of the supernatant was added back to the neuronal cultures, which were first washed carefully with warm DPBS if the well contained substantial debris. Then conditioned medium from microglia (100 µl), which had been prepared from wild-type, $Asc^{-/-}$ or $Nlrp3^{-/-}$ mice (see section 2.2.4), was added to the neuronal cultures.

The plates were incubated for 24 h, each well was washed with cold PBS, and residual buffer was removed using a vacuum suction system. Cells were lysed with 30 µl cold RIPA buffer [50 mM Tris-HCl (pH 8.0), 300 mM NaCl, 1% deoxycholic acid, 2% Triton X-100, 1% SDS, 50 mM EDTA, 50 mM sodium fluoride, protease inhibitor cocktail], and the plates were incubated on ice on a shaker for up to 5 min. Then 10 µl of 4 x loading buffer [0.2 M Tris-HCl (pH 8.0), 0.4 M DTT, 8% SDS, 6 mM Bromophenol blue, 4.3 M Glycerol] was added, and the mixture was transferred to a new tube, heated at 95 °C for 5 min, and either stored at -20 °C until use or immediately fractionated by SDS-PAGE for western blotting. Tau and kinases/phosphatase levels were detected in these samples with the antibodies listed in section 2.1.6.

2.2.9 Isolation of sarkosyl-soluble and -insoluble tau

To analyze levels of tau, kinases and phosphatase in mouse brain, isolation of sarkosyl-soluble and -insoluble tau was performed (Fig. 9). Frozen hippocampi were weighed and homogenized in 10 volumes of H buffer [10 mM Tris-HCl (pH 8), 1 mM EGTA, 800 mM NaCl, 10% sucrose, 0.1 mM PMSF, 1 mM sodium orthovanadate, 1x protease/phosphatase inhibitor] using a Precellys device at a speed of 5000 rpm for one cycle of 20 seconds. The homogenate was centrifuged for 20 min at 21,000 g at 4 °C, and the supernatant was transferred to a clean tube. The pellet was extracted and centrifuged as above, and the supernatant was combined with the previous one. The pellet was homogenized by 15 passages through a 1/2-inch, 27G needle (attached to a 1-ml syringe) in 20 volumes of RIPA buffer. The homogenized pellet was used for the analysis of membrane-bound proteins such as CaMKIIα. The pooled supernatant was supplemented with 1% sarkosyl and incubated for 2 h at 37 °C. Equal volumes were centrifuged for 1 h at 300,000 g at 20 °C, and the supernatant containing sarkosyl-soluble tau was collected and stored at -80 °C. The pellet containing sarkosyl-insoluble tau was homogenized by pipetting up and down with H buffer containing 1% sarkosyl, then centrifuging for 30 min at 300,000 g at 20 °C. The pellet was resuspended in 1x loading buffer, heated for 5 min at 95 °C and stored at -80 °C.

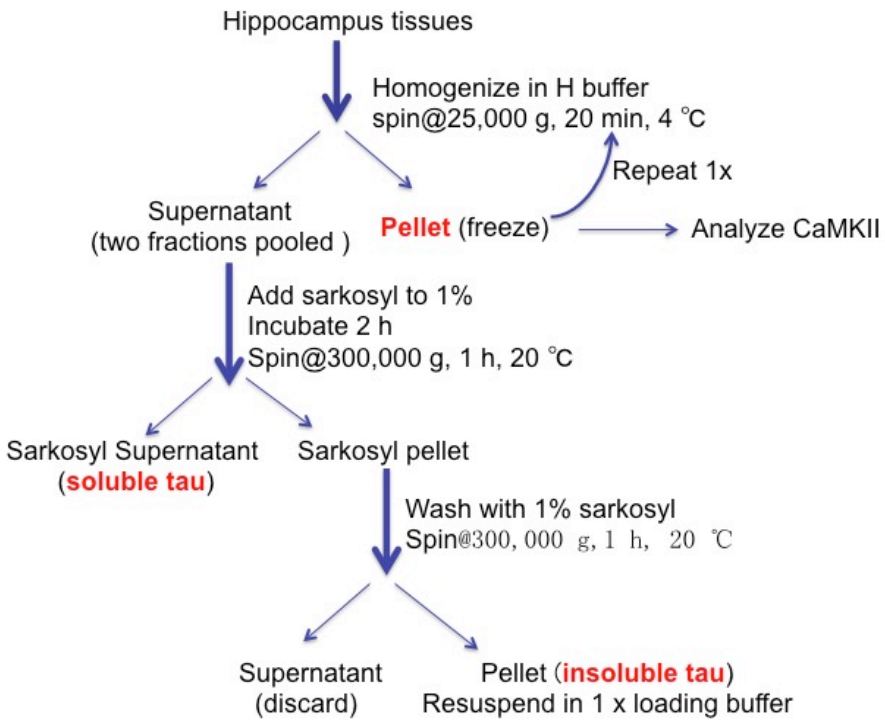

Fig. 9: Scheme of isolation of sarkosyl-soluble and -insoluble tau

2.2.10 Immunoblotting

Total protein concentrations were estimated using a BCA kit. According to the manufacturer's instructions, equal amounts of protein (in the case of brain lysates) or equal sample volumes (in the case of neuronal lysates) were mixed with 4x loading buffer to a final concentration of 1x loading buffer and heated for 5 min at 95 °C. The proteins were fractionated on 4-12% Bis-Tris NuPAGE Novex gels, which were run in 1x MES buffer. Proteins were wet-transferred to nitrocellulose membrane in transfer buffer (1x Tris-glycine, 20% methanol), and the membrane was blocked for at least 30 min with 3% BSA in 1x TBS [20 mM Tris (pH 7.6), 0.15 M NaCl], followed by incubation overnight at 4 °C with primary antibodies in 3% BSA in TBS-Tween (1x Tris-buffered saline, 0.1% Tween 20). The membrane was washed three times (5 min each) in TBS-Tween wash buffer. Proteins were visualized using fluorescently tagged secondary antibodies, which were incubated with the membrane in 3% BSA in TBS-Tween for 40 min. After three washes in

TBS-Tween buffer, blots were imaged using an ODYSSEY CLx system, and bands were quantified using ImageStudio. All loading controls were run on the same gel as the respective experimental samples.

2.2.11 Immunohistochemical staining

In each experiment, at least three serial brain sections (40 µm thick) were analyzed from each animal (Ising et al. 2019). Staining was performed in a free-floating format, and staining was visualized using 3-3'-diaminobenzidine (DAB), fluorescently-tagged antibodies or thioflavin S.

For DAB staining, sections were washed for 5 min in TBS at RT. Then they were sequentially incubated in hydrogen peroxide (0.3%) for 10 min at RT, blocked with 3% milk in 0.25% TBS-X (1x TBS with Triton-X100), washed three times (5 min each) in TBS, and incubated with a biotinylated AT8 antibody in 1% milk overnight at 4 °C. After triple times washes, sections were processed using the VECTASTAIN® Elite ABC Peroxidase kit, followed by incubation in ABC Elite in TBS for 1 h at RT. After three times washes, they were developed in DAB solution. The staining lasted for fewer than 20 min, and the intensity of the staining was checked several times during its development to avoid saturation. Sections were washed three times, mounted on glass slides and dried overnight in a fume hood at RT. Finally, slides were dehydrated through a graded series of ethanol solutions, followed by a solution of xylene (Table 3).

Table 3 Steps in the dehydration of brain sections after DAB staining

Step	Solution	Duration of incubation (min)
1	50% ethanol	1
2	70% ethanol	1
3	95% ethanol	1
4	95% ethanol	1
5	95% ethanol	1

6	100% ethanol	1
7	100% ethanol	1
8	Xylene	4
9	Xylene	4

The slides were taken out of xylene, a small amount of Cytoseal 60 mounting medium was applied to the bottom of the slide, and the cover glass was added very slowly to avoid generating bubbles. The slides were dried on a flat surface overnight in a fume hood at RT, then imaged under a 10x objective on a slide scanner (AxioScan.Z1). ImageJ/FiJi software was used for threshold analysis.

For immunofluorescence staining to detect pSer416-Tau and for staining with thioflavine S, sections were mounted on a slide, dried overnight at RT washed three times with PBS, rinsed in Milli-Q water, and incubated at 37 °C for 10 min. Then pepsin solution (1 mg/ml pepsin, 0.2 M HCl) was added to the sections, which were incubated for another 10 min at 37 °C. Sections were washed three times, blocked for 30 min with 3% BSA in PBSX (1x PBS with 0.1% Triton-X100), incubated with antibody against pTau-Ser416 at 4 °C overnight, washed three times with PBS, incubated with Alexa555-conjugated secondary antibody in 3% BSA/PBSX for 1 h at RT, then finally washed another three times.

During the next staining steps, a slide carrier wrapped with aluminum foil was used to ensure rapid processing and to avoid light exposure. Sections were soaked in Milli-Q water for 1 min, incubated in 0.1% Sudan Black in 70% EtOH for 20 min, washed for 4 min, and incubated in 0.025% thioflavine S in 50% EtOH for 5 min. Finally, sections were washed three times quickly in 50% ethanol and three times for longer in Milli-Q water, after which a small amount of Prolong Gold + DAPI was added, and the coverslip was placed on top.

Images of intact hippocampi were taken using a Nikon eclipse Ti under a 20x objective. Images of all sections were processed using ImageJ and Adobe

Photoshop CS5.

2.2.12 Statistics and reproducibility

In descriptions of data, n refers to the number of independent biological samples. Data were analyzed using GraphPad Prism, and all data were presented as mean ± standard error of the mean (SEM). Differences among the groups were assessed for significance using one-way ANOVA, followed by Tukey's test or unpaired two-tailed t-test. Results were statistically significant if $P < 0.05$.

3. Results

3.1 Tau pathology is reduced in inflammasome-knockout mice

To evaluate whether the NLRP3 inflammasome is related to pathogenesis in tauopathies, we immunostained mouse hippocampi from 11-month-old Tau22, Tau22/Asc$^{-/-}$ and Tau22/Nlrp3$^{-/-}$ mice with an antibody detecting tau phosphorylated at Ser202 and Thr 205 (clone AT8). Tau22 mice are used as a model of frontotemporal dementia. They overexpress mutated forms of human tau, leading to tau aggregation in intracellular NFTs and spatial memory deficits (Schindowski et al. 2006).

Compared to Tau22 mice, Tau22/Asc$^{-/-}$ mice showed a trend towards lower levels of phospho-tau in the hippocampus, while Tau22/Nlrp3$^{-/-}$ mice of the same age showed significantly lower levels (Fig. 10). Both knockout strains showed significantly lower levels of phospho-tau in the CA1 region than Tau22 mice.

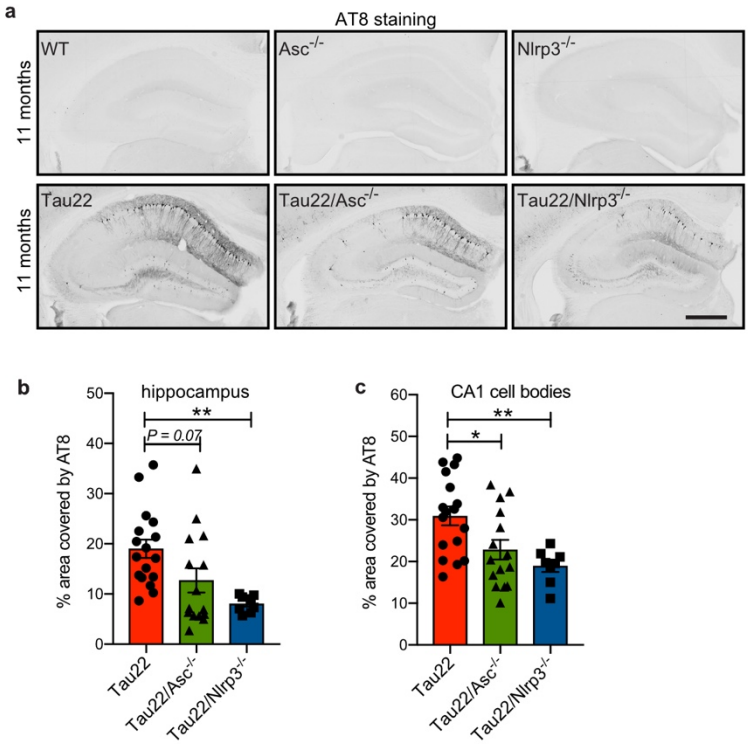

Fig. 10: Lower levels of phospho-tau in inflammasome-knockout mice. Brain sections from 11-month-old mice were immunostained for phosphorylated tau using the AT8 antibody. **(a)** Representative immunohistochemical staining of

hippocampus. Scale bar, 500 µm. **(b,c)** Quantification of percentages of area staining positive for AT8 in hippocampus or CA1 region. Data are mean ± SEM (n=17 in Tau22, n=15 in Tau22/Asc$^{-/-}$ and n=8 in Tau22/Nlrp3$^{-/-}$), and significance was tested using one-way ANOVA followed by Tukey's test. For hippocampal staining, **P=0.0055. For CA1 region staining, *P=0.0278 and **P=0.0059. WT, wild-type. Adapted from (Ising et al. 2019).

Under normal conditions, tau is highly soluble, whereas in tauopathies, it can be misfolded and aggregate (Wang and Mandelkow 2016). Sarkosyl-soluble fractions of hippocampi from 11-month-old mice were analyzed using the MC1 antibody to assess the presence of misfolded tau (Davies 2000). Tau22/Asc$^{-/-}$ and Tau22/Nlrp3$^{-/-}$ mice contained lower levels of misfolded tau than Tau22 mice (Fig. 11), even though the three mouse strains expressed similar levels of total tau. These results suggest milder tau pathology in aged inflammasome-knockout mice.

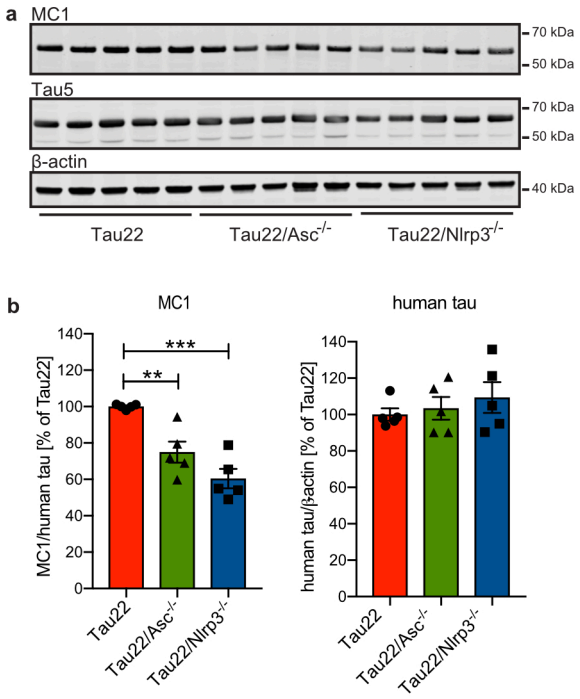

Fig. 11: Lower levels of misfolded Tau in the sarkosyl-soluble fraction of hippocampi from inflammasome-knockout mice. Fractions from 11-month-old mice were immunoblotted using MC1 antibody to detect misfolded tau or Tau5 antibody to detect total tau. **(a)** Representative immunoblot results. **(b)** Quantification. Data are mean ± SEM (n = 5 per group), and significance was

tested using one-way ANOVA, followed by Tukey's test. **P=0.0056, ***P=0.0001. Adapted from (Ising et al. 2019).

3.2 The NLRP3 inflammasome regulates kinases and phosphatases

Protein kinases such as GSK-3, CDK5 and PKA as well as phosphatases such as PP2A regulate tau phosphorylation (Iqbal et al. 2005) and may therefore affect risk of AD. The activity of several of these factors was assessed in hippocampi from Tau22, Tau22/Asc$^{-/-}$ and Tau22/Nlrp3$^{-/-}$ mice. PP2A activity was evaluated based on levels of its demethylated subunit C and levels of its negative regulator PME-1 (Ortega-Gutierrez et al. 2008). GSK-3β activity was measured based on levels of enzyme phosphorylated at Tyr216.

Tau22 mice showed similar hippocampal levels of active phosphatase PP2A, PME and GSK-3β as wild-type animals (Fig. 12). Tau22/Asc$^{-/-}$ and Tau22/Nlrp3$^{-/-}$ mice showed higher hippocampal levels of active PP2A and lower levels of PME-1 than Tau22 mice (Fig. 13a-c). In addition, Tau22/Nlrp3$^{-/-}$ mice showed lower GSK-3β activity than Tau22 mice (Fig. 13a,d).

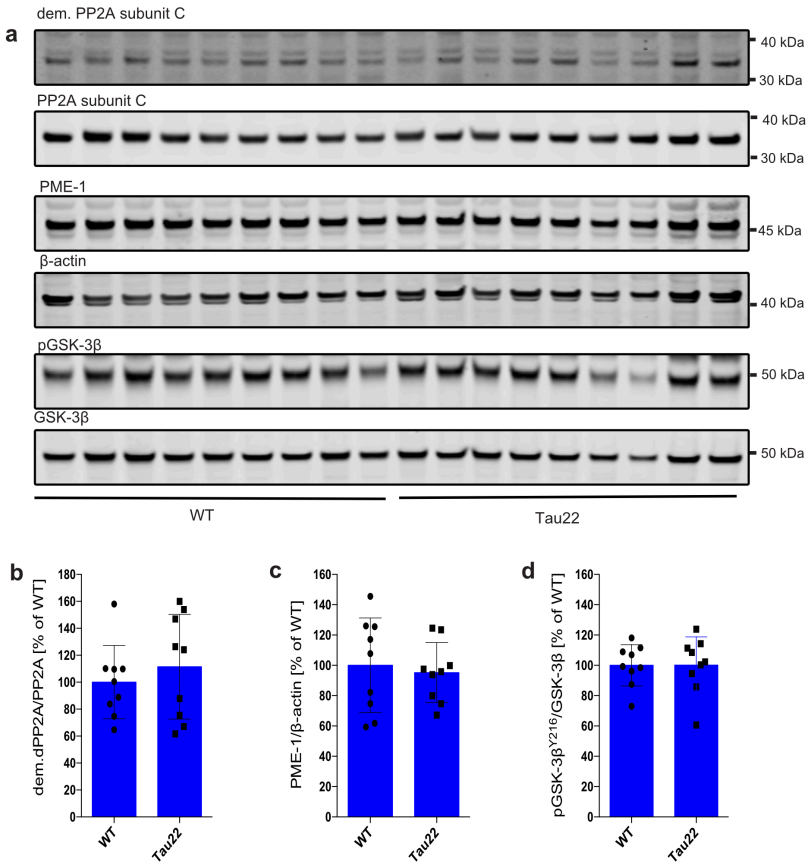

Fig. 12: Wild-type levels of PP2A phosphatase, phosphatase inhibitor PME-1 and GSK-3β kinase in Tau22 mice. Fractions from 11-month-old Tau22 or wild-type (WT) mice were immunoblotted against demethylated PP2A subunit C (dem. PP2A), total PP2A subunit C, PP2A methylesterase PME-1, GSK-3β phosphorylated at Tyr216, and total GSK-3β. **(a)** Representative immunoblotting results. **(b-d)** Quantification. Data are mean ± SEM (n=9 for each group), and significance was tested using unpaired two-tailed t-test. dem, demethylated.

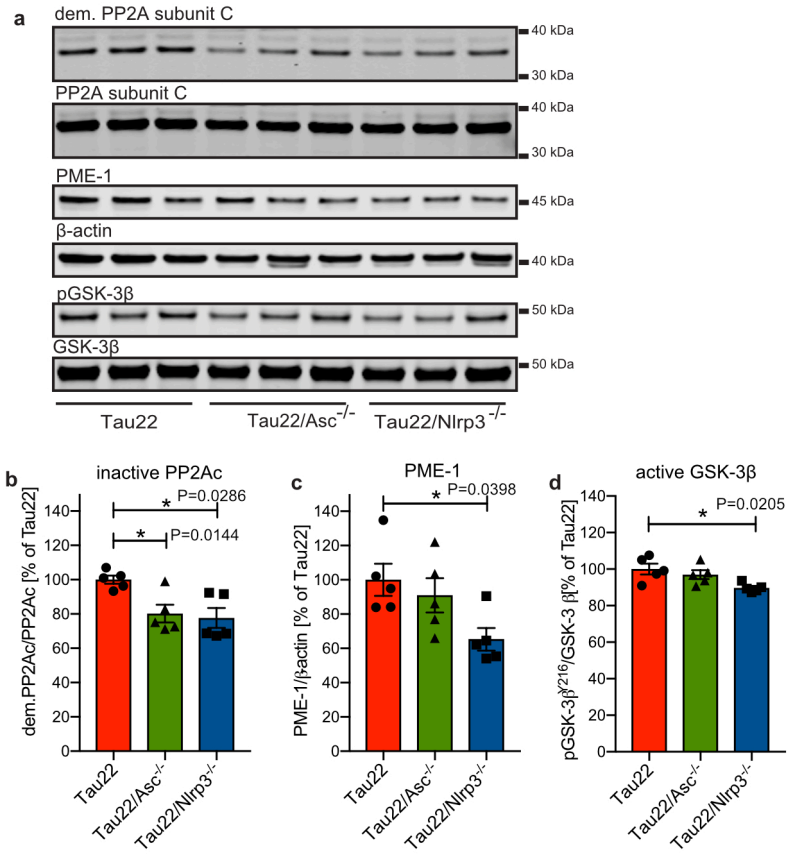

Fig. 13: Deficiency of NLRP3 or ASC promotes PP2A activity in mice. Hippocampal lysates from 11-month-old Tau22 or knockout mice were immunoblotted as described in Fig. 12. **(a)** Representative immunoblotting results. **(b-d)** Quantification. Data are mean ± SEM (n=5 for each group), and significance was tested using one-way ANOVA, followed by Tukey's test. dem. PP2A, demethylated PP2A subunit C; PME-1, PP2A methylesterase; pGSK-3β, GSK-3β phosphorylated at Tyr216. Adapted from (Ising et al. 2019).

CDK5 and p38 kinases are involved in tau pathology (Pei et al. 2001; Pei et al. 1998), so the activity of these kinases was assessed in hippocampus. The activity of CDK5 was measured in terms of the ratio of its two regulatory proteins, p25 and p35. The activity of p38 was measured in terms of levels of the phosphorylated active form (p-p38). Tau22 and Tau22/Nlrp3$^{-/-}$ mice showed similar levels of active CDK5 and p38 (Fig. 14). These results suggest that neither CDK5 nor p38 are involved in NLRP3-regulated tau pathology in our mouse model.

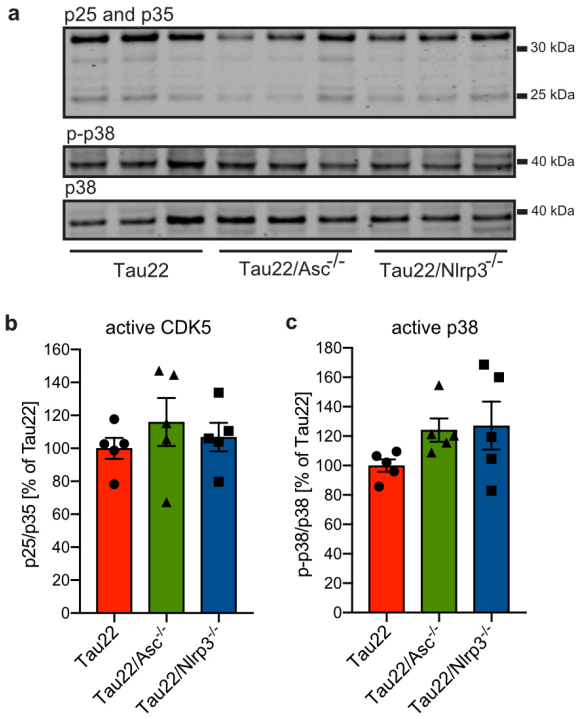

Fig. 14: Deficiency of NLRP3 or ASC does not alter activity of CDK5 or p38 in mice. Hippocampal lysates from 11-month-old Tau22 or knockout mice were immunoblotted against two regulators of CDK kinase (p25 and p35) and the total and active phosphorylated forms of p38 (p-p38). **(a)** Representative immunoblotting results. **(b-d)** Quantification. Data are mean ± SEM (n=5 for each group), and significance was tested using one-way ANOVA, followed by Tukey's test. CDK5, cyclin-dependent protein kinase-5. Adapted from (Ising et al. 2019).

3.3 Knock out of *Nlrp3* or *Asc* reduces CaMKII kinase activity and tau phosphorylation

CaMKII, which contains subunits α, β, and γ, plays an important role in the abnormal hyperphosphorylation of tau (Iqbal et al. 2005). Here, the α subunit of CaMKII (CaMKIIα) in hippocampus of mice was analyzed using antibodies to detect total subunit as well as the subunit autophosphorylated on Thr286 (Barkai et al. 2000), which indicates activation of the enzyme. Tau22 mice tended to show greater hippocampal CaMKII activity than wild-type animals, but the difference did not achieve significance (Fig. 15a-b). Tau22/Asc$^{-/-}$ and Tau22/Nlrp3$^{-/-}$ mice showed significantly lower CaMKII activity in hippocampus than Tau22 animals (Fig. 15c-d). These results indicate downregulation of CaMKII activity in the absence of NLRP3.

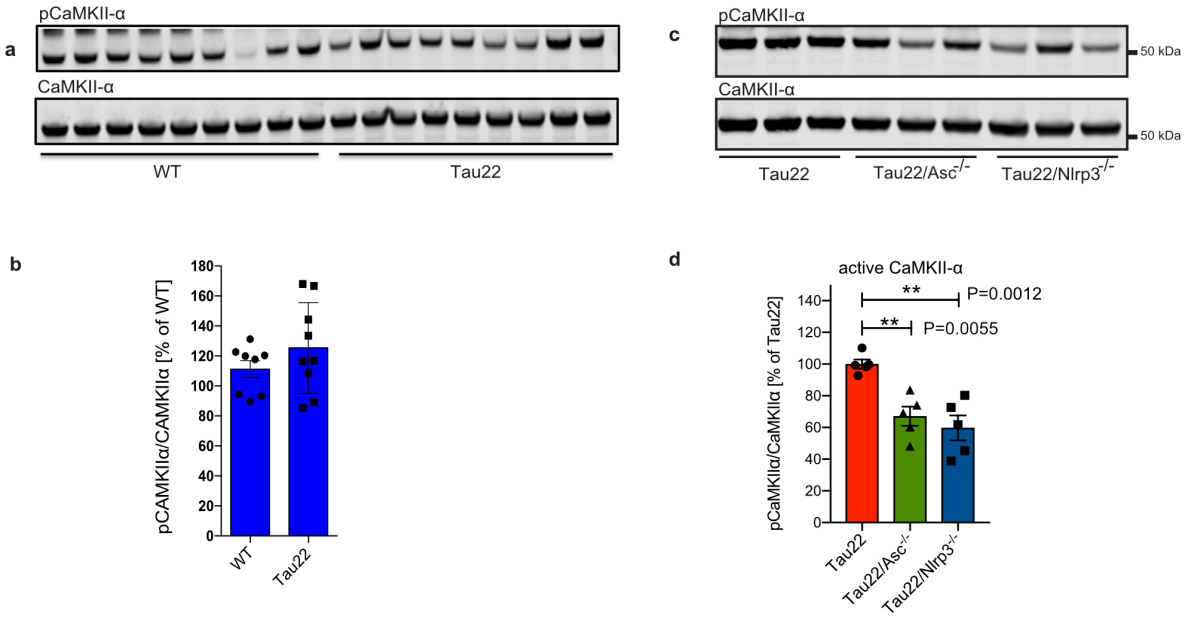

Fig. 15: Deficiency of NLRP3 or ASC inhibits CaMKII kinase activity in mice. Hippocampal lysates from 11-month-old wild-type (WT), Tau22 or knockout mice were immunoblotted against total CaMKII subunit α (CaMKIIα) or CaMKIIα autophosphorylated at Thr286 (pCaMKIIα). **(a,c)** Representative immunoblotting results. **(b)** Quantification of experiments represented in panel (a). Data are mean ± SEM (n=8 for WT, after removal of one outlier; n=9 for Tau22), and significance was tested using unpaired two-tailed t-test. Difference between the two groups: P = 0.2523. **(d)** Quantification of experiments represented in panel (c). Data are mean ± SEM (n=5 for each group), and significance was tested using one-way ANOVA, followed by Tukey's test. CaMKII, Calmodulin dependent protein kinase II. Adapted from (Ising et al. 2019).

Next, whether the decreased CaMKII activity translated to tau phosphorylation was explored, based on the ability of CaMKII to phosphorylate tau at Ser416. Tau22/Asc$^{-/-}$ and Tau22/Nlrp3$^{-/-}$ mice showed significantly smaller CA1 areas that were positive for tau-pSer416 than Tau22 mice (Fig. 16). This suggests lower tau phosphorylation in the absence of the NLRP3 inflammasome, which may reflect lower CaMKII activity.

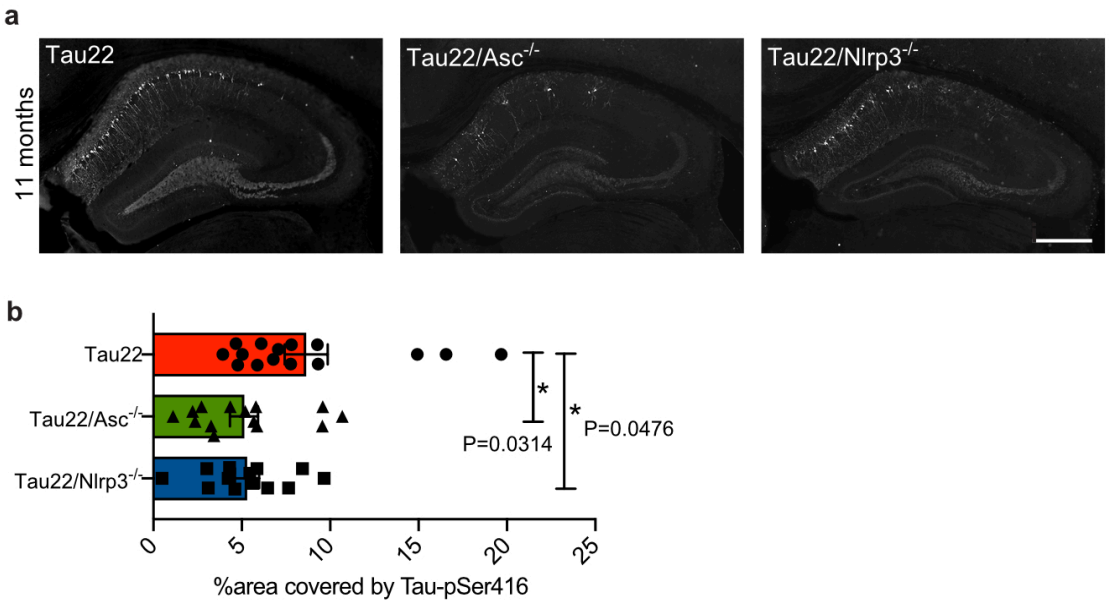

Fig. 16: Deficiency of Nlrp3 or ASC reduces tau phosphorylation at Ser416 in the CA1 region of mice. Hippocampal sections from 11-month-old mice were immunostained against Tau-pSer416. **(a)** Representative immunostained micrographs. Scale bar, 500 µm. **(b)** Quantification in the CA1 region. Data are mean ± SEM [Tau22 (n=15); Tau22/Asc$^{-/-}$ (n=14); Tau22/Nlrp3$^{-/-}$ (n=13)], and significance was tested using one-way ANOVA, followed by Tukey's test. Adapted from (Ising et al. 2019).

3.4 The NLRP3 inflammasome regulates kinase activity and tau phosphorylation *in vitro*

To elucidate the molecular pathways leading to the tau regulation that we observed in Asc$^{-/-}$ and Nlrp3$^{-/-}$ mice, we turned to *in vitro* experiments conducted with primary cultures. Primary microglial cultures were prepared from wild-type, Asc$^{-/-}$ and Nlrp3$^{-/-}$ mice, then they were primed using LPS and activated using ATP, leading to the assembly of the NLRP3 inflammasome. The medium of these microglial cultures was collected as conditioned medium and applied to primary cultures of mouse hippocampal neurons (Fig. 17). NLRP3 inflammasome activation was confirmed in the conditioned medium by assaying IL-1β levels (Fig. 18). As expected, IL-1β in conditioned medium from wild-type microglia averaged over 50,000 pg/ml, higher than the concentration in conditioned medium from

Asc$^{-/-}$ or Nlrp3$^{-/-}$ microglia.

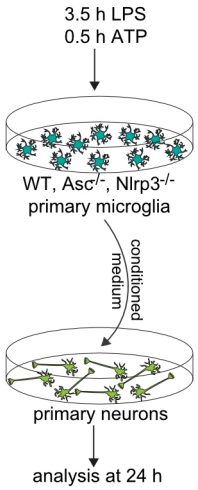

Fig. 17: Schematic of the experimental set-up used for *in vitro* experiments. LPS, lipopolysaccharide; WT, wild-type. Adapted from (Ising et al. 2019).

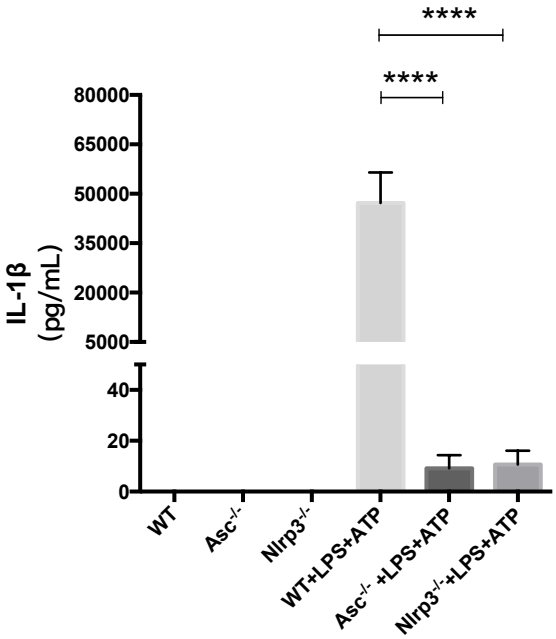

Fig. 18: Concentration of IL-1β in conditioned medium from primary microglial cultures from wild-type (WT) and transgenic mice. In some cases, microglial cultures have been primed with lipopolysacchride (LPS) and activated with ATP. Data are mean ± SEM (n=4 for Nlrp3$^{-/-}$, n=7 for all other strains), and significance was tested using one-way ANOVA followed by Tukey's test. ****P < 0.0001.

Treating primary hippocampal neurons with conditioned medium from Asc$^{-/-}$ or Nlrp3$^{-/-}$ microglia led to lower levels of tau phosphorylated at Ser396 and Ser404,

as detected using anti-PHF-1 antibody, than treating the neurons with conditioned medium from wild-type microglia (Fig. 19a). These lower levels of tau phosphorylation were associated with lower levels of total tau as detected using anti-tau5 antibody (Fig. 19b). The decreased levels of phosphor-tau were also related with lower levels of active CaMKII, as showed using anti-pCaMKIIα antibody which detects CaMKII subunit autophosphorylated on Thr286 (Fig. 19c). These *in vitro* findings support the idea that activation of the NLRP3 inflammasome contributes to CaMKII upregulation, and that lack of a functional NLRP3 inflammasome reduces tau pathology.

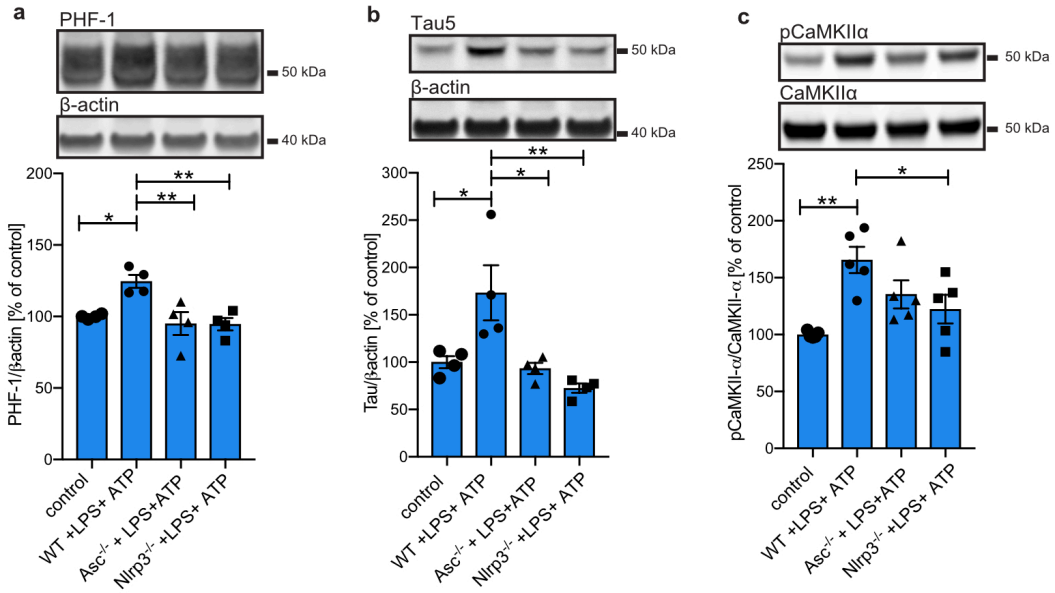

Fig. 19: The NLRP3 inflammasome promotes abnormal tau formation and CaMKII activity *in vitro*. Primary hippocampal neurons were cultured in conditioned medium from microglia from wild-type (WT) or transgenic mice. The microglia had been primed (or not) with lipopolysaccharide and activated with ATP before harvest of the conditioned medium. The neuronal cultures were analyzed by immunoblotting against **(a)** tau phosphorylated at Ser396 and Ser404 (PHF-1), **(b)** total tau or **(c)** CaMKII subunit α autophosphorylated at Thr286 (pCaMKIIα). Data are mean ± SEM [n=4 for panels (a)-(b), n=5 for panel (c)]. Significance was tested using one-way ANOVA, followed by Tukey's test. In panel (a): Control vs. WT+ATP: *P=0.0235, WT+ATP vs. $Asc^{-/-}$+ATP: **P=0.0072, WT+ATP vs. $Nlrp3^{-/-}$+ATP: **P=0.0064. In panel (b): Control vs. WT+ATP: *P=0.0252, WT+ATP vs. $Asc^{-/-}$+ATP: *P=0.0148, WT+ATP vs. $Nlrp3^{-/-}$+ATP: **P=0.0029. In panel (c): **P=0.0022, *P=0.0454. Adapted from (Ising et al. 2019).

3.5 The inflammasome inhibits CaMKII activity via the IL-1 receptor and downstream effectors

Next, we asked whether IL-1β in the conditioned medium, secreted as a result of NLRP3 inflammasome activation, regulated CaMKII activity in the primary hippocampal neurons. Primary neurons were pretreated with an antibody antagonist of the IL-1 receptor (IL-1R) or its corresponding isotype control antibody IgG, then incubated in conditioned medium from wild-type microglia that had been primed with LPS and activated with ATP. Inhibiting IL-1R antagonized the ability of the conditioned medium to activate CaMKII (Fig. 20a), as did inhibiting IRAK4 or MEK1/2, which are downstream effectors in the IL-1β signaling pathway (Fig. 20b). These findings indicate that microglia-derived IL-1β exacerbates tau pathology by upregulating CaMKII, just as it upregulates other tau kinases (Bhaskar et al. 2010).

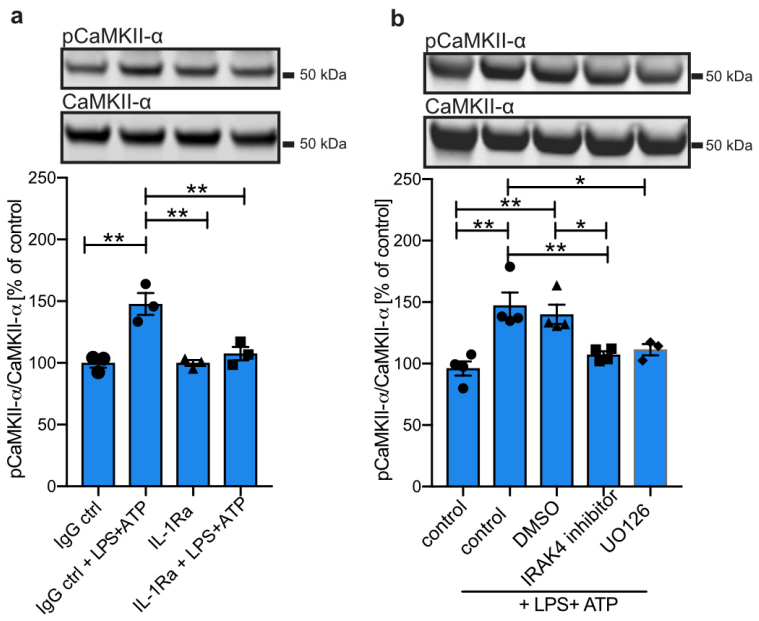

Fig. 20: The IL-1 receptor and its downstream effectors activate CaMKII in hippocampal neurons. (a) Primary hippocampal neurons were pretreated with an IL-1 receptor antagonist (IL-1Ra) or its corresponding isotype control, followed by conditioned medium from wild-type (WT) microglia that had been primed with lipopolysaccharide (LPS) and activated with ATP. Neuronal lysates were immunoblotted against CaMKII subunit α autophosphorylated at Thr286 (pCaMKIIα). Data are mean ± SEM (n=3), and significance was tested using one-way ANOVA followed by Tukey's test. IgG ctrl vs. IgG ctrl+ATP: **P=0.0015, IgG ctrl+ATP vs. IL-1ra+ATP: **P=0.0044. **(b)** Primary hippocampal neurons were

treated and analyzed as described in panel (a), except that they were pretreated with DMSO, an IRAK4 inhibitor or the MEK1/2 inhibitor UO126. Data are mean ± SEM (n=3 for UO126, n=4 for all other groups), and significance was tested as in panel (a). Ctrl vs. ctrl+ATP: **P=0.0011; ctrl vs. DMSO+ATP: **P=0.0040; ctrl+ATP vs. IRAK4 inhibitor+ATP: **P=0.0087; ctrl+ATP vs. UO126+ATP: *P=0.0309; DMSO+ATP vs. IRAK4 inhibitor: *P=0.0338. Adapted from (Ising et al. 2019).

3.6 ASC specks induce tau pathology

ASC specks have been reported to contribute to the propagation of inflammasome activation (Baroja-Mazo et al. 2014) and to exacerbation of amyloid pathology (Venegas et al. 2017). To investigate the ability of ASC specks to induce tau pathology and explore a potential mediating role for the NLRP3 inflammasome, we used an injection model based on a previously published study (Venegas et al. 2017). Tau-transgenic mice with or without a functional NLRP3 inflammasome were injected with ASC specks in one hippocampus and with vehicle in the contralateral one (Fig. 21).

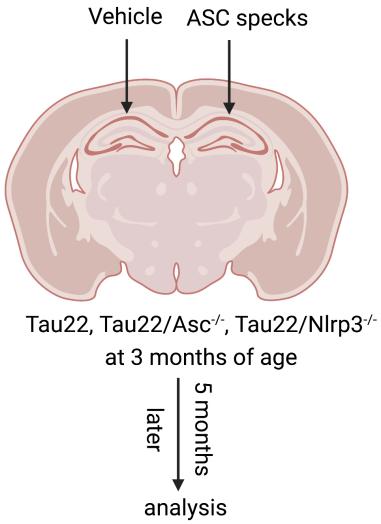

Fig. 21: Schematic of the injection model.

After injection, brains were sectioned and stained for hyperphosphorylated tau using AT8 antibody or for aggregated tau using thioflavine S. Injection of ASC specks efficiently increased tau aggregation in the CA1 region of Tau22 mice, but not Tau22/Asc$^{-/-}$ or Tau22/Nlrp3$^{-/-}$ mice (Fig. 22). Similarly, injection of ASC specks efficiently induced tau hyperphosphorylation in the CA1 region in Tau22 mice, but not Tau22/Nlrp3$^{-/-}$ animals (Fig. 23). These results suggest that ASC specks induce intraneuronal tau pathology, to which the NLRP3 inflammasome contributes.

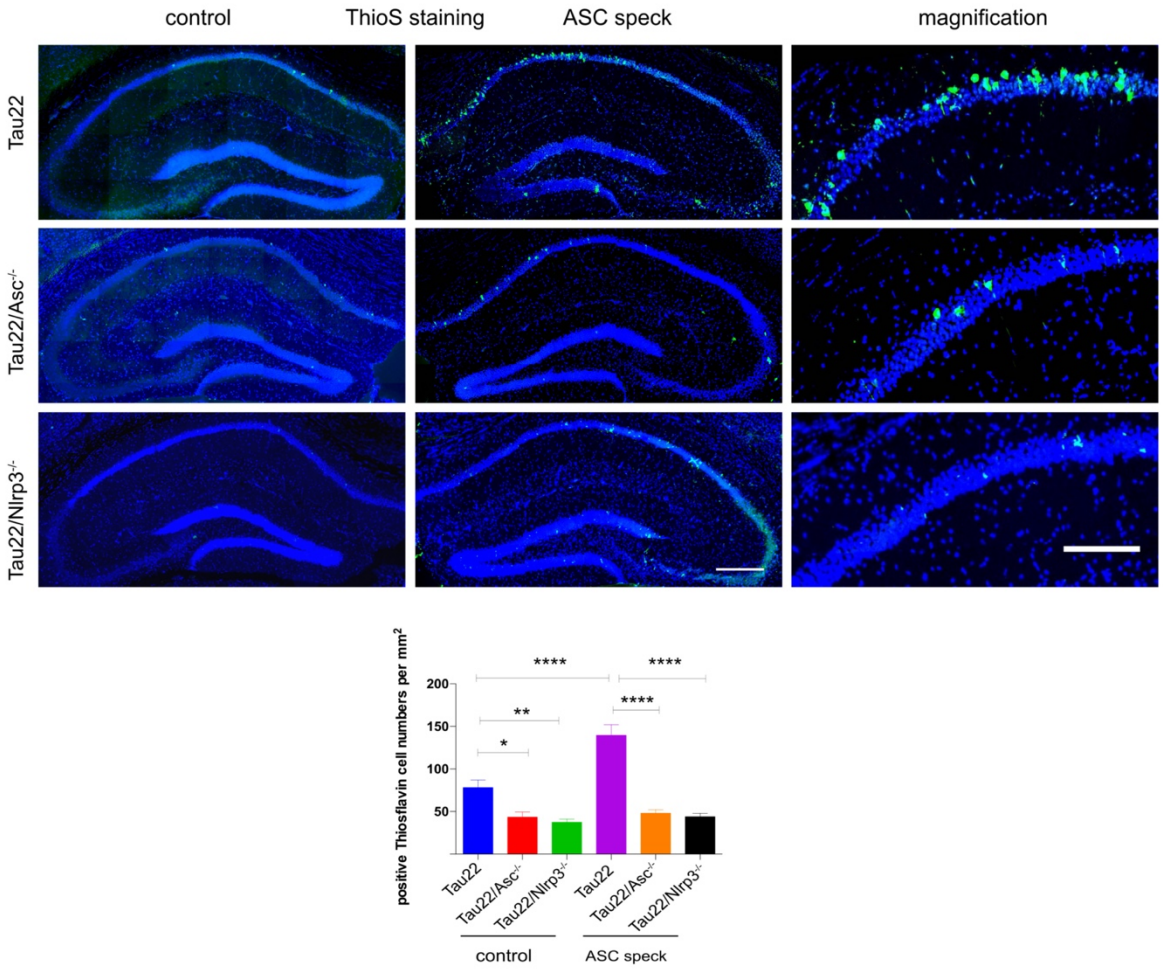

Fig. 22: Injection of ASC specks leads to tau aggregation in mice only in the presence of a functional NLRP3 inflammasome. Mice were injected with ASC specks directly in one hippocampus and with vehicle in the contralateral one. 5 months later, brains were sectioned and stained for aggregated Tau using thioflavine S. **(a)** Representative micrographs of stained hippocampus. Scale bar, 500 µm (middle) or 250 µm (right). **(b)** Quantification of thioflavine S-positive cells

in the CA1 region. Data are mean ± SEM (n=7 animals and 46 sections for Tau22, n=5 animals and 40 sections for Tau22/Asc$^{-/-}$, n=5 animals and 50 sections for Tau22/Nlrp3$^{-/-}$), and significance was tested by one-way ANOVA followed by Tukey's test. ****P<0.0001, **P < 0.01, *P < 0.05.

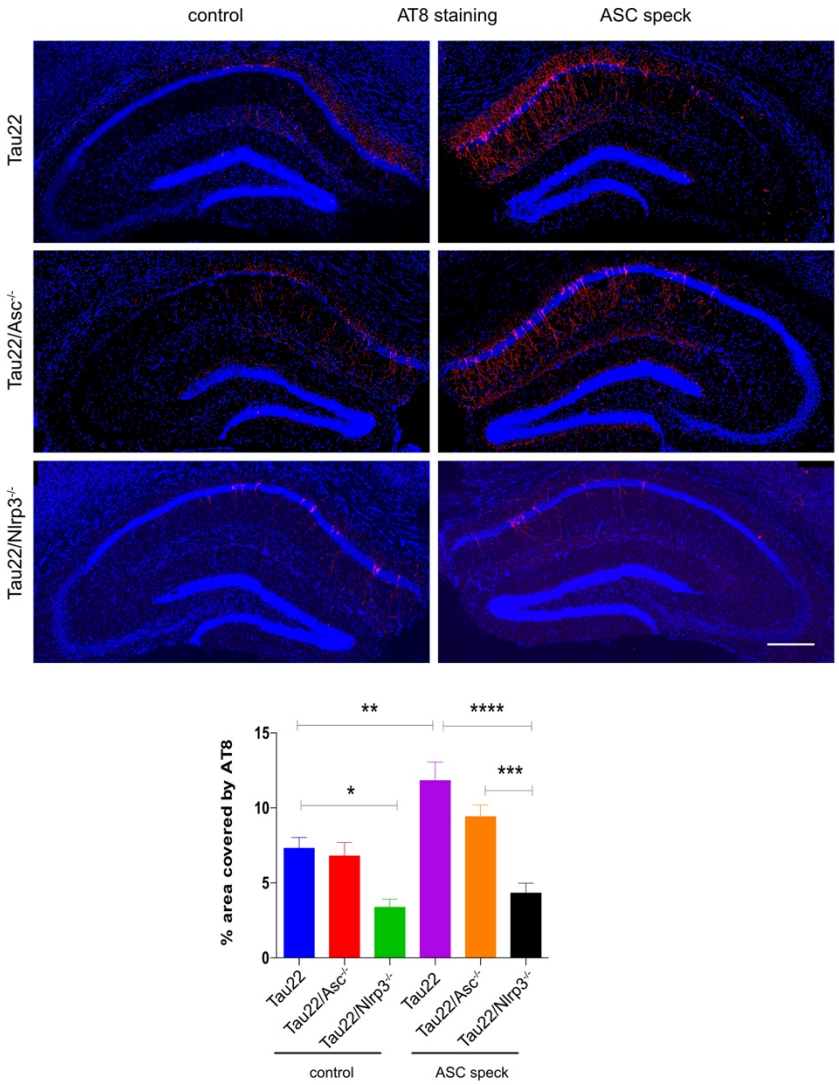

Fig. 23: Injection of ASC specks leads to tau hyperphosphorylation in mice. Mice were injected with ASC specks directly in one hippocampus and with vehicle in the contralateral one. 5 months later, brains were sectioned and stained for hyperphosphorylated tau using antibody AT8. **(a)** Representative micrographs of stained hippocampus. Scale bar, 500 µm. **(b)** Quantification of the percentage of area stained by AT8 in the CA1 region. Data are mean ± SEM (n=7 animals and 46 sections for Tau22, n=5 animals and 40 sections for Tau22/Asc$^{-/-}$, n=5 animals and 50 sections for Tau22/Nlrp3$^{-/-}$), and significance was tested using one-way ANOVA with Tukey's test. ****P<0.0001, ***P<0.001, **P < 0.01, *P < 0.05.

4. Discussion

4.1 NLRP3 activation links amyloid-β deposition and tau pathology

4.1.1 The amyloid hypothesis

The amyloid hypothesis (Hardy and Higgins 1992) is widely accepted as the explanation for the pathogenesis of AD. It stipulates that Aβ deposition is the major initiator of AD pathogenesis, driving all pathophysiological events, including NFT formation, inflammation, synaptic dysfunction and neurodegeneration. This hypothesis stems from findings in the 1980s that Aβ was the main pathological component in amyloid plaques from patients with AD or Down syndrome (Glenner and Wong 1984). Indeed, the gene encoding Aβ lies on chromosome 21, the trisomy of which causes Down syndrome (Goldgaber et al. 1987; Kang et al. 1987). The amyloid hypothesis may not, however, tell the complete story because therapeutic strategies targeting Aβ have failed to prevent cognitive decline or improve cognitive parameters in large clinical trials (Karran, Mercken, and De Strooper 2011). These results suggest that targeting Aβ production alone might not be enough to stop pathogenesis.

Several lines of evidence have linked Aβ aggregation and tau pathology. In patients with clinical dementia, the severity of Aβ aggregation strongly correlates with tau pathology (Brier et al. 2016). Mouse models support the idea that Aβ deposits exacerbate tau pathology. In fact, intracerebral injection of Aβ fibrils or Aβ-rich brain homogenate can also induce tau pathology in tau-transgenic mice (Bolmont et al. 2007; Gotz et al. 2001). Aβ can activate tau kinases (Cho and Johnson 2004). Increasing Aβ load in mouse models of AD exacerbates tau toxicity in neurons and cognitive deficit (Billings et al. 2005). These studies indicate that Aβ deposition is the upstream event of tau aggregation.

More recent work has refined the amyloid hypothesis into the Aβ-tau cascade hypothesis (Hardy and Selkoe 2002; Jack et al. 2013; Jack et al. 2010), which stipulates that Aβ, tau and neuroinflammation interact to contribute to AD.

Activated microglia, reactive astrocytes and enhanced levels of proinflammatory factors, which are characteristics of neuroinflammation, may affect Aβ clearance or deposition and promote tau pathology (Gallardo and Holtzman 2019). Accumulated Aβ and NFTs together with the chronic neuroinflammation may result in progressive neuronal loss, leading to declined cognition and memory loss (Ising and Heneka 2018).

4.1.2 Amyloid-β accumulation and NLRP3 activation promote each other

Fibrillar Aβ has been shown *in vitro* to interact with the NLRP3 inflammasome and contribute to its activation (Halle et al. 2008). That study showed that fibrillar Aβ induced IL-1β release from microglia via a mechanism dependent on NLRP3 and ASC. Incubating the microglia with a caspase-1 inhibitor reduced IL-1β production. These findings are consistent with the idea that Aβ phagocytosis activates the NLRP3-caspase-1 pathway, impairing lysosomes, inducing cathepsin B leakage into the cytosol and increasing IL-1β release. Not only fibrillar Aβ but also soluble Aβ induces NLRP3 inflammasome activation via a mechanism requiring the CD36 receptor on the surface of macrophages (Sheedy et al. 2013).

Work with transgenic mice supports the idea that the NLRP3 inflammasome and IL-1β contribute to Aβ deposition and AD pathogenesis. When APP/PS1 transgenic mice were crossed with Nlrp3$^{-/-}$ or caspase 1$^{-/-}$ animals, the progeny showed no detectable cleaved caspase-1, indicating inactive NLRP3 inflammasomes; lower IL-1β levels and Aβ plaque load in the brain; and improved spatial memory (Heneka et al. 2013). The significant decrease in Aβ deposition was not due to altered APP processing but instead to high phagocytic activity. That study indicated that the absence of just one component of the NLRP3 pathway can reduce amyloid load; induce microglia to adopt a phagocytic, anti-inflammatory phenotype; and improve cognitive function.

A role for NLRP3 in Aβ pathology has been confirmed in studies involving pharmacological NLRP3 inhibitors (Coll et al. 2015; Dempsey et al. 2017). The

selective NLRP3 inhibitor MCC950 reduced IL-1β production in mouse bone marrow- and human monocyte-derived macrophages (Coll et al. 2015). It also stimulated phagocytosis of Aβ by microglia in culture, and it reduced Aβ accumulation and improved cognitive function in APP/PS1 mice (Dempsey et al. 2017).

ASC specks form fibrillar ASC aggregates upon inflammasome activation. They contribute to the propagation of inflammasome activation in a prion-like way. ASC specks are involved in Aβ deposition from an early phase, binding to Aβ and aggravating amyloid pathology (Venegas et al. 2017). In primary cultures of mouse microglia, ASC-Aβ complexes, which mimic the clustering of Aβ around ASC fibrils, activated the NLRP3 inflammasome to a stronger extent than ASC or Aβ alone (Friker et al. 2020). ASC-Aβ complexes also impaired Aβ clearance. These findings suggest that Aβ clustering around ASC fibrils amplifies their toxicity to microglia.

Taken together, previous work from our group and others suggests that Aβ aggregates activate the NLRP3 inflammasome, which inhibits Aβ clearance and promotes its deposition. This leads to a vicious cycle that ultimately destroys neuronal function. In this background, we investigated the links between activation of the NLRP3 inflammasome and tau pathology.

4.1.3 NLRP3 activation induces tau pathology

Like AD, frontotemporal dementia is a neurodegenerative disease involving tau pathology, including NFTs. Therefore we analyzed NLRP3 inflammasome activation in Tau22 mice, which serve as a model of frontotemporal dementia (Schindowski et al. 2006).

Reducing NLRP3 levels in Tau22 mice reduced levels of hyperphosphorylated tau (Fig. 10) and aggregated tau (Fig. 11) in the hippocampus and CA1 region. Eliminating ASCs from the animals exerted similar effects, but to a weaker extent.

To validate the association between NLRP3 and tau pathology *in vitro*, hippocampal neurons expressing human tau were cultured in conditioned medium from primary microglia that had been isolated from wild-type, $Asc^{-/-}$ or $Nlrp3^{-/-}$ mice and then primed with LPS and stimulated with ATP. Conditioned medium from either knockout strain led to lower tau phosphorylation and lower total tau levels (Fig.19). These findings support our *in vivo* observations that deficiency of the NLRP3 inflammasome alleviates tau phosphorylation and aggregation.

Patients with frontotemporal dementia show elevated levels of ASC, cleaved caspase-1 and mature IL-1β in the brain, indicating activation of the NLRP3 inflammasome (Ising et al. 2019). In addition, treating primary microglia with brain homogenate from Tau22 mice induced secretion of IL-1β (Ising et al. 2019). That study also showed that exposing primary microglia to tau monomers and oligomers enhanced IL-1β secretion through a mechanism dependent on ASC and NLRP3, while also stimulating release of cleaved caspase-1. Whether fibrils exert the same effects is unclear, since studies have reported conflicting results: tau fibrils did not significantly affect NLRP3 activation in one study (Ising et al. 2019), while they promoted such activation in another (Stancu et al. 2019).

Altogether, the present work and the literature support an important role for activation of the NLRP3 inflammasome in tau pathology, consistent with the amyloid-tau hypothesis of AD.

4.2 Possible mechanisms of NLRP3 inflammasome on tau pathology

4.2.1 NLRP3 regulates kinases and phosphatase involved in tau pathology

One possible explanation for the therapeutic effects of NLRP3 deficiency in reducing tau pathology is altered activity of tau kinases and phosphatases. We demonstrated in mice that NLRP3 upregulated the tau kinases GSK-3β (Fig. 13) and CaMKII (Fig. 15), while downregulating PP2A and upregulating its inhibitor PME-1 (Fig. 13). Knocking out the NLRP3 from mice reduced CaMKII-mediated phosphorylation of tau at Ser416 (Fig. 16). Consistently, conditioned medium from

microglia lacking the NLRP3 inflammasome led to lower CaMKII activity in primary hippocampal neurons (Fig. 19). These results implicate CaMKII kinase in NLRP3-mediated tau pathology.

Although there is no initial increase in tau kinases and PP2A enzyme activity in Tau22 mice (Fig. 12 and Fig. 15), the deficiency of NLRP3 inflammasome has a beneficial role in tau pathology in our mice model. One reason might be that a transient change of tau kinase or phosphatase level was not detected by western blot in the 11-month-old Tau22 mice. It's reported that transient upregulation of tau kinases, such as CaMKII, would be sufficient to induce abnormal tau phosphorylation, despite that the activities of the protein kinases have not been shown to be upregulated in AD brains reproducibly (Iqbal et al. 2005).

4.2.2 NLRP3 activation induces tau pathology in part via IL-1β

To explore the molecular pathway through which NLRP3 activation upregulates CaMKII, we focused on the IL-1 receptor, since the NLRP3 inflammasome cleaves pro-IL-1β into active IL-1β. We found that culturing primary hippocampal neurons in conditioned medium from wild-type primary microglia that had been primed with LPS and activated with ATP upregulated CaMKIIα activity, but this upregulation was much weaker when the IL-1 receptor was inhibited (Fig. 20). We observed similar effects when we inhibited not the IL-1 receptor but its downstream effector IRAK4 or MEK1/2. These results suggest that NLRP3 regulates CaMKIIα activity through the IL-1β signaling pathway. It may help explain why overexpression of IL-1β in aged transgenic mice can exacerbate tau pathology (Ghosh et al. 2013). This regulation may also help explain why tau hyperphosphorylation requires activation of the IL-1 receptor (Bhaskar et al. 2010). In this study, the hyperphosphorylation of tau also required IL-1β-driven p38 mediated signal transduction in hTau mice lacking the microglial-specific fractalkine receptor (Bhaskar et al. 2010). While we demonstrate the p38 kinase level remained unchaged in Tau22 mice lack of NLRP3 inflammasome (Fig. 14). The different mouse models and study design used might explain the discrepancy.

Indeed, this link between NLRP3 and CaMKIIα may help explain the association between microglial activation and tauopathies (Bhaskar et al. 2010; Cho et al. 2015; Ghosh et al. 2013; Kitazawa et al. 2005; Lee et al. 2010; Li et al. 2003). Treating transgenic mice with LPS induces systemic inflammation, which in turn activates microglia, ultimately leading to tau hyperphosphorylation (Kitazawa et al. 2005). Conversely, tau pathology is attenuated by suppressing microglial activation, whether by using the immunosuppressor FK506 (Yoshiyama et al. 2007), knocking out the microglial receptor CX3CR1 (Bhaskar et al. 2010), or reducing the numbers of microglia (Asai et al. 2015).

We demonstrated that stimulating primary hippocampal neurons with conditioned medium from $Asc^{-/-}$ or $Nlrp3^{-/-}$ microglia led to lower tau phosphorylation and accumulation than with medium from wild-type microglia. These findings further support an important role for IL-1β signaling in tau pathology.

4.3 ASC specks exacerbate tau pathology via an NLRP3-dependent mechanism

We demonstrated that injection of ASC specks in hippocampus induced tau hyperphosphorylation and aggregation in the hippocampus of Tau22 mice, but not Tau22/$Asc^{-/-}$ or Tau22/$Nlrp3^{-/-}$ mice (Figs. 22-23). These results indicate that extracellular ASC specks might induce intraneuronal pathology. They also indicate essential roles for NLRP3 activity and ASC in ASC speck-induced tau pathology.

Extracellular ASC specks may induce intracellular tau pathology by stimulating inflammatory responses. Extracellular ASC specks act as an endogenous danger signal, triggering the cleavage of pro-IL-1β into active IL-1β and its release from macrophages (Franklin et al. 2014). That study also showed that injection of ASC specks into the ears of wild-type mice caused acute inflammatory reactions. Future work should confirm that extracellular ASC specks induce intracellular tau pathology, and they should explore the underlying mechanisms, which might be due to effects of ASC specks on neurons directly or via microglia indirectly.

Future experiments should also address whether ASC specks interact with tau. Previous work *in vitro* and *in vivo* already showed that ASC specks interact with Aβ and induce Aβ aggregation (Venegas et al. 2017). That work confirmed that ASC binds Aβ and promotes Aβ aggregation in APP/PS1 mice, and that ASC specks induce Aβ aggregation *in vitro* in a time- and dose-dependent manner.

Our work demonstrates the important role of NLRP3 activity in ASC speck-induced tau pathology, and the role of ASC in tau aggregation. Our results extend a previous study in which injecting brain lysate from APP/PS1 mice into other APP/PS1 mice induced Aβ deposition, but not when the recipient animals lacked the ASC gene or when anti-ASC antibody was co-injected with the lysate (Venegas et al. 2017). Similarly, another study reported that intrahippocampal injection of brain lysate from APP/PS1 mice into Tau22 mice induced hyperphosphorylated tau formation in the CA1 region, but not when the recipient animals lacked the Asc or Nlrp3 gene (Ising et al. 2019). This literature and the present work suggest important roles for NLRP3 and ASC in the Aβ-tau cascade hypothesis.

4.4 Future therapeutic in Alzheimer's disease

Several previous studies identified the NLRP3 inflammasome as a mediator of Aβ pathology by showing that (1) aggregates of Aβ activate the NLRP3 inflammasome (Halle et al. 2008), (2) deficiency of the NLRP3 inflammasome inhibits amyloid pathology (Heneka et al. 2013), and (3) ASC specks induce cross-seeding of amyloid pathology (Venegas et al. 2017). In the present work, we show that activation of NLRP3 drives Aβ-induced tau pathology in Tau22 mice. In addition to the literature, our results add new insights into how NLRP3 activation affects tau phosphorylation and aggregation. Our work helps define how NLRP3 activation links Aβ and tau pathology via ASC specks, offering novel targets for intervention in AD.

In addition to AD, NLRP3 may be a therapeutic target in various autoimmune and

autoinflammatory diseases, such as rheumatoid arthritis (Lamkanfi and Dixit 2012; Vande Walle et al. 2014). Besides, NLRP3 has been reported to be associated with the pathogenesis of metabolic disorders, including type 2 diabetes, obesity, atherosclerosis and gout (Wen, Ting, and O'Neill 2012).

The NLRP3 inhibitor MCC950 has been shown to attenuate the symptoms of experimental autoimmune encephalomyelitis. And MCC950 also reduced neonatal lethality of cryopyrin-associated periodic syndrome in a mouse model (Coll et al. 2015). The beneficial effects of MCC950 in some mouse models of NLRP3-related diseases seem not to involve direct inhibition of interactions of the NLRP3 inflammasome with other NLRP3 inflammasomes or with ASC (Coll et al. 2015; Dempsey et al. 2017). Thus, MCC950 may inhibit the NLRP3 inflammasome by targeting an unknown upstream signaling event.

Other treatments for NLRP3-related diseases include biologicals targeting IL-1 (Dinarello, Simon, and van der Meer 2012). These agents may be less appropriate for treating NLRP3-related diseases than inhibitors of the NLRP3 inflammasome. These diseases involve not only IL-1β but also IL-18 and other proinflammatory factors. In addition, IL-1β can be generated by pathways involving other types of inflammasomes or even no inflammasomes at all (Davis, Wen, and Ting 2011; Netea et al. 2015). Thus, inhibiting the NLRP3 inflammasome may lead to less immunosuppression than inhibiting IL-1β function.

4.5 Summary of findings

Here we investigated how the NLRP3 inflammasome contributes to the development and progression of tau pathology. We demonstrated that (1) genetically inhibiting NLRP3 activity in Tau22 mice reduced tau phosphorylation and aggregation in different brain regions. (2) This effect was due to the ability of microglial NLRP3 to regulate neuronal tau kinases GSK-3β and CaMKIIα, as well as tau phosphatase PP2A and its upstream regulator PME-1. (3) Conditioned medium from microglia stimulated tau phosphorylation and CaMKIIα activity in

primary hippocampal neurons to a smaller extent when the microglia lacked the NLRP3 inflammasome. (4) Blocking the IL-1 receptor prevented the NLRP3 inflammasome from upregulating CaMKIIα activity, as did blocking downstream effectors of the IL-1 receptor, IRAK4 and MEK1/2. (5) Injecting ASC specks in hippocampus induced tau hyperphosphorylation and aggregation in Tau22 mice, but not Tau22/Asc$^{-/-}$ or Tau22/Nlrp3$^{-/-}$ mice. These results show that activation of the NLRP3 inflammasome plays an important role in the development of tau pathology, in part potentially by acting as a bridge between Aβ deposition and tau pathology. Our findings support and help define the Aβ-tau cascade hypothesis.

5. Abstract

Alzheimer's disease (AD) is characterized by the extracellular accumulation of amyloid beta (Aβ), intraneuronal formation of neurofibrillary tangles composed of hyperphosphorylated tau, and activation of microglia, which are the innate immune cells of the brain. Aβ activates microglia to induce NLRP3, ASC and caspase-1 to assemble into the NLRP3 inflammasome. This complex stimulates the production and secretion of inflammatory mediators such as IL-1β and ASC specks.

Here we investigated how the NLRP3 inflammasome contributes to the development and progression of tau pathology. Knockout of Asc or Nlrp3 from mice expressing human tau ("Tau22 mice") reduced the activity of the tau kinases CaMKII and GSK-3β while promoting the activity of the tau phosphatase PP2A. This strongly protected mice from accumulation of hyperphosphorylated, misfolded tau. These protective effects were stronger in the absence of NLRP3 than in the absence of ASC. We confirmed these protective effects *in vitro* by incubating primary hippocampal neurons from Tau22 mice in conditioned medium from primary microglia that had been isolated from wild-type, $Nlrp3^{-/-}$ or $Asc^{-/-}$ mice and stimulated with LPS and ATP. Conditioned medium from microglia lacking NLRP3 or ASC led to less tau phosphorylation and accumulation as well as lower CaMKII activity in the hippocampal neurons. Inhibition of the IL-1 receptor or its downstream effectors IRAK4 or MEK1/2 protected the neurons from these effects. Injecting ASC specks directly into the hippocampus induced tau hyperphosphorylation and aggregation in Tau22 mice, but not Tau22/$Asc^{-/-}$ or Tau22/$Nlrp3^{-/-}$ mice. These results suggest that NLRP3 acts via IL-1β signaling to drive tau pathology and potentially also link tauopathy with Aβ pathology.

This work supports the hypothesis that innate immune activation contributes to tau pathology. In Alzheimer's disease, early Aβ deposition may induce NLRP3-mediated innate immune responses that lead to tau pathology and neuronal demise. Furthermore, this works shows that NLRP3 inflammasome activations also play a direct role in tauopathies independent of Aβ. In this way, the present work may help to develop new therapies against the disease.

6. List of figures

7. List of tables

8. References

Ajami B, Bennett JL, Krieger C, Tetzlaff W, Rossi FM. Local self-renewal can sustain CNS microglia maintenance and function throughout adult life. Nat Neurosci 2007; 10: 1538-1543

Alonso AC, Zaidi T, Grundke-Iqbal I, Iqbal K. Role of abnormally phosphorylated tau in the breakdown of microtubules in Alzheimer disease. Proc Natl Acad Sci U S A 1994; 91: 5562-5566

Alzheimer's, Association. 2020 Alzheimer's disease facts and figures. Alzheimers Dement 2020; 16: 391-460

Asai H, Ikezu S, Tsunoda S, Medalla M, Luebke J, Haydar T, Wolozin B, Butovsky O, S. Kugler, Ikezu T. Depletion of microglia and inhibition of exosome synthesis halt tau propagation. Nat Neurosci 2015; 18: 1584-1593

Askew K, Li K, Olmos-Alonso A, Garcia-Moreno F, Liang Y, Richardson P, Tipton T, Chapman MA, Riecken K, Beccari S, Sierra A, Molnar Z, Cragg MS, Garaschuk O, V. H. Perry, Gomez-Nicola D. Coupled Proliferation and Apoptosis Maintain the Rapid Turnover of Microglia in the Adult Brain. Cell Rep 2017; 18: 391-405

Barkai U, Prigent-Tessier A, Tessier C, Gibori GB, Gibori G. Involvement of SOCS-1, the suppressor of cytokine signaling, in the prevention of prolactin-responsive gene expression in decidual cells. Mol Endocrinol 2000; 14: 554-563

Baroja-Mazo A, Martin-Sanchez F, Gomez AI, Martinez CM, Amores-Iniesta J, Compan V, Barbera-Cremades M, Yague J, Ruiz-Ortiz E, Anton J, Bujan S, Couillin I, Brough D, Arostegui JI, Pelegrin P. The NLRP3 inflammasome is released as a particulate danger signal that amplifies the inflammatory response. Nat Immunol 2014; 15: 738-748

Bennecib M, Gong CX, Grundke-Iqbal I, Iqbal K. Inhibition of PP-2A upregulates CaMKII in rat forebrain and induces hyperphosphorylation of tau at Ser 262/356.

FEBS Lett 2001; 490: 15-22

Bertram L, Lill CM, Tanzi RE. The genetics of Alzheimer disease: back to the future. Neuron 2010; 68: 270-281

Bhaskar K, Konerth M, Kokiko-Cochran ON, Cardona A, Ransohoff RM, Lamb BT. Regulation of tau pathology by the microglial fractalkine receptor. Neuron 2010; 68: 19-31

Billings LM, Oddo S, Green KN, McGaugh JL, LaFerla FM. Intraneuronal Abeta causes the onset of early Alzheimer's disease-related cognitive deficits in transgenic mice. Neuron 2005; 45: 675-688

Bolmont T, Clavaguera F, Meyer-Luehmann M, Herzig MC, Radde R, Staufenbiel M, Lewis J, Hutton M, Tolnay M, Jucker M. Induction of tau pathology by intracerebral infusion of amyloid-beta-containing brain extract and by amyloid-beta deposition in APP x Tau transgenic mice. Am J Pathol 2007; 171: 2012-2020

Breitner JC. The role of anti-inflammatory drugs in the prevention and treatment of Alzheimer's disease. Annu Rev Med 1996; 47: 401-411

Brier MR, Gordon B, Friedrichsen K, McCarthy J, Stern A, Christensen J, Owen C, Aldea P, Su Y, Hassenstab J, Cairns NJ, Holtzman DM, Fagan AM, Morris JC, Benzinger TL, Ances BM. Tau and Abeta imaging, CSF measures, and cognition in Alzheimer's disease. Sci Transl Med 2016; 8: 338ra66

Broderick L, Hoffman HM. cASCading specks. Nat Immunol 2014; 15: 698-700

Cho JH, Johnson GV. Glycogen synthase kinase 3 beta induces caspase-cleaved tau aggregation in situ. J Biol Chem 2004; 279: 54716-54723

Cho SH, Chen JA, Sayed F, Ward ME, Gao F, Nguyen TA, Krabbe G, Sohn PD, Lo I, Minami S, Devidze N, Zhou Y, Coppola G, Gan L. SIRT1 deficiency in microglia contributes to cognitive decline in aging and neurodegeneration via epigenetic regulation of IL-1beta. J Neurosci 2015; 35: 807-818

Coll RC, Robertson AA, Chae JJ, Higgins SC, Munoz-Planillo R, Inserra MC, I. Vetter I, Dungan LS, Monks BG, Stutz A, Croker DE, Butler MS, Haneklaus M, Sutton CE, Nunez G, Latz E, Kastner DL, Mills KH, Masters SL, Schroder K, Cooper MA, O'Neill LA. A small-molecule inhibitor of the NLRP3 inflammasome for the treatment of inflammatory diseases. Nat Med 2015; 21: 248-255

Cruz JC, Tsai LH. Cdk5 deregulation in the pathogenesis of Alzheimer's disease. Trends Mol Med 2004; 10: 452-8

Davies P. Characterization and use of monoclonal antibodies to tau and paired helical filament tau. Methods Mol Med 2000; 32: 361-373

Davis BK, Wen H, Ting JP. The inflammasome NLRs in immunity, inflammation, and associated diseases. Annu Rev Immunol 2011; 29: 707-35

Davis S, Laroche S. What can rodent models tell us about cognitive decline in Alzheimer's disease? Mol Neurobiol 2003; 27: 249-276

Dempsey C, Rubio Araiz A, Bryson KJ, Finucane O, Larkin C, Mills EL, Robertson AAB, Cooper MA, O'Neill LAJ, Lynch MA. Inhibiting the NLRP3 inflammasome with MCC950 promotes non-phlogistic clearance of amyloid-beta and cognitive function in APP/PS1 mice. Brain Behav Immun 2017; 61: 306-316

Dostert C, Petrilli V, Van Bruggen R, Steele C, Mossman BT, Tschopp J. Innate immune activation through Nalp3 inflammasome sensing of asbestos and silica. Science 2008; 320: 674-677

Duff K, Knight H, Refolo LM, Sanders S, Yu X, Picciano M, Malester B, Hutton M, Adamson J, Goedert M, Burki K, Davies P. Characterization of pathology in transgenic mice over-expressing human genomic and cDNA tau transgenes. Neurobiol Dis 2000; 7: 87-98

Duncan JA, Bergstralh DT, Wang Y, Willingham SB, Ye Z, Zimmermann AG, Ting JP. Cryopyrin/NALP3 binds ATP/dATP, is an ATPase, and requires ATP binding to

mediate inflammatory signaling. Proc Natl Acad Sci U S A 2007; 104: 8041-8046

Franklin BS, Bossaller L, De Nardo D, Ratter JM, Stutz A, Engels G, Brenker C, Nordhoff M, Mirandola SR, Al-Amoudi A, Mangan MS, Zimmer S, Monks BG, Fricke M, Schmidt RE, Espevik T, Jones B, Jarnicki AG, Hansbro PM, Busto P, Marshak-Rothstein A, Hornemann S, Aguzzi A, Kastenmuller W, Latz E. The adaptor ASC has extracellular and 'prionoid' activities that propagate inflammation. Nat Immunol 2014; 15: 727-737

Friker LL, Scheiblich H, Hochheiser IV, Brinkschulte R, Riedel D, Latz E, Geyer M, Heneka MT. beta-Amyloid Clustering around ASC Fibrils Boosts Its Toxicity in Microglia. Cell Rep 2020; 30: 3743-54 e6

Gallardo G, Holtzman DM. Amyloid-beta and Tau at the Crossroads of Alzheimer's Disease. Adv Exp Med Biol 2019; 1184: 187-203

Ghosh S, Wu MD, Shaftel SS, Kyrkanides S, LaFerla FM, Olschowka JA, O'Banion MK. Sustained interleukin-1beta overexpression exacerbates tau pathology despite reduced amyloid burden in an Alzheimer's mouse model. J Neurosci 2013; 33: 5053-5064

Ginhoux F, Prinz M. Origin of microglia: current concepts and past controversies. Cold Spring Harb Perspect Biol 2015; 7: a020537

Glenner GG, Wong CW. Alzheimer's disease and Down's syndrome: sharing of a unique cerebrovascular amyloid fibril protein. Biochem Biophys Res Commun 1984; 122: 1131-5

Goedert M, Spillantini MG. Pathogenesis of the tauopathies. J Mol Neurosci 2011; 45: 425-431

Goldgaber D, Lerman MI, McBride OW, Saffiotti U, Gajdusek DC. Characterization and chromosomal localization of a cDNA encoding brain amyloid of Alzheimer's disease. Science 1987; 235: 877-80

Gotz J, Chen F, van Dorpe J, Nitsch RM. Formation of neurofibrillary tangles in P301l tau transgenic mice induced by Abeta 42 fibrils. Science 2001; 293: 1491-1495

Grundke-Iqbal I, Iqbal K, Tung YC, Quinlan M, Wisniewski HM, Binder LI. Abnormal phosphorylation of the microtubule-associated protein tau (tau) in Alzheimer cytoskeletal pathology. Proc Natl Acad Sci U S A 1986; 83: 4913-4917

Guerreiro R, Wojtas A, Bras J, Carrasquillo M, Rogaeva E, Majounie E, Cruchaga C, Sassi C, Kauwe JS, Younkin S, Hazrati L, Collinge J, Pocock J, Lashley T, Williams J, Lambert JC, Amouyel P, Goate A, Rademakers R, Morgan K, Powell J, St George-Hyslop P, Singleton A, Hardy J, Group Alzheimer Genetic Analysis. TREM2 variants in Alzheimer's disease. N Engl J Med 2013; 368: 117-127

Guo H, Callaway JB, Ting JP. Inflammasomes: mechanism of action, role in disease, and therapeutics. Nat Med 2015; 21: 677-687

Halle A, Hornung V, Petzold GC, Stewart CR, Monks BG, Reinheckel T, Fitzgerald KA, Latz E, Moore KJ, Golenbock DT. The NALP3 inflammasome is involved in the innate immune response to amyloid-beta. Nat Immunol 2008; 9: 857-965

Hanger DP, Betts JC, Loviny TL, Blackstock WP, Anderton BH. New phosphorylation sites identified in hyperphosphorylated tau (paired helical filament-tau) from Alzheimer's disease brain using nanoelectrospray mass spectrometry. J Neurochem 1998; 71: 2465-2476

Hardy JA, Higgins GA. Alzheimer's disease: the amyloid cascade hypothesis. Science 1992; 256: 184-185

Hardy J, Selkoe DJ. The amyloid hypothesis of Alzheimer's disease: progress and problems on the road to therapeutics. Science 2002; 297: 353-356

Heneka MT. Inflammasome activation and innate immunity in Alzheimer's disease. Brain Pathol 2017; 27: 220-222

Heneka MT, Carson MJ, El Khoury J, Landreth GE, Brosseron F, Feinstein DL, Jacobs AH, Wyss-Coray T, Vitorica J, Ransohoff RM, Herrup K, Frautschy SA, Finsen B, Brown GC, Verkhratsky A, Yamanaka K, Koistinaho J, Latz E, Halle A, Petzold GC, Town T, Morgan D, Shinohara ML, Perry VH, Holmes C, Bazan NG, Brooks DJ, Hunot S, Joseph B, Deigendesch N, Garaschuk O, Boddeke E, Dinarello CA, Breitner JC, Cole GM, Golenbock DT, Kummer MP. Neuroinflammation in Alzheimer's disease. Lancet Neurol 2015; 14: 388-405

Heneka MT, Golenbock DT, Latz E. Innate immunity in Alzheimer's disease. Nat Immunol 2015; 16: 229-236

Heneka MT, Kummer MP, Latz E. Innate immune activation in neurodegenerative disease. Nat Rev Immunol 2014; 14: 463-477

Heneka MT, Kummer MP, Stutz A, Delekate A, Schwartz S, Vieira-Saecker A, Griep A, Axt D, Remus A, Tzeng TC, Gelpi E, Halle A, Korte M, Latz E, Golenbock DT. NLRP3 is activated in Alzheimer's disease and contributes to pathology in APP/PS1 mice. Nature 2013; 493: 674-678

Heneka MT, McManus RM, Latz E. Inflammasome signalling in brain function and neurodegenerative disease. Nat Rev Neurosci 2018; 19: 610-21

Iba M, Guo JL, McBride JD, Zhang B, Trojanowski JQ, Lee VM. Synthetic tau fibrils mediate transmission of neurofibrillary tangles in a transgenic mouse model of Alzheimer's-like tauopathy. J Neurosci 2013; 33: 1024-1037

in t' Veld BA, Ruitenberg A, Hofman A, Launer LJ, van Duijn CM, Stijnen T, Breteler MM, Stricker BH. Nonsteroidal antiinflammatory drugs and the risk of Alzheimer's disease. N Engl J Med 2001; 345: 1515-1521

Iqbal K, Alonso Adel C, Chen S, Chohan MO, El-Akkad E, Gong CX, Khatoon S, Li B, Liu F, Rahman A, Tanimukai H, Grundke-Iqbal I. Tau pathology in Alzheimer disease and other tauopathies. Biochim Biophys Acta 2005; 1739: 198-210

Ising C, Heneka MT. Functional and structural damage of neurons by innate immune mechanisms during neurodegeneration. Cell Death Dis 2018; 9: 120

Ising C, Venegas C, Zhang S, Scheiblich H, Schmidt SV, Vieira-Saecker A, Schwartz S, Albasset S, McManus RM, Tejera D, Griep A, Santarelli F, Brosseron F, Opitz S, Stunden J, Merten M, Kayed R, Golenbock DT, Blum D, Latz E, Buee L, Heneka MT. NLRP3 inflammasome activation drives tau pathology. Nature 2019; 575: 669-673

Iwashyna TJ, Ely EW, Smith DM, Langa KM. Long-term cognitive impairment and functional disability among survivors of severe sepsis. JAMA 2010; 304: 1787-1794

Jack CR, Knopman DS, Jagust WJ, Petersen RC, Weiner MW, Aisen PS, Shaw LM, Vemuri P, Wiste HJ, Weigand SD, Lesnick TG, Pankratz VS, Donohue MC, Trojanowski JQ. Tracking pathophysiological processes in Alzheimer's disease: an updated hypothetical model of dynamic biomarkers. Lancet Neurol 2013; 12: 207-216

Jack CR, Knopman DS, Jagust WJ, Shaw LM, Aisen PS, Weiner MW, Petersen RC, Trojanowski JQ. Hypothetical model of dynamic biomarkers of the Alzheimer's pathological cascade. Lancet Neurol 2010; 9: 119-128

Jana M, Palencia CA, Pahan K. Fibrillar amyloid-beta peptides activate microglia via TLR2: implications for Alzheimer's disease. J Immunol 2008; 181: 7254-7262

Jicha GA, Berenfeld B, Davies P. Sequence requirements for formation of conformational variants of tau similar to those found in Alzheimer's disease. J Neurosci Res 1999; 55: 713-723

Jicha GA, Rockwood JM, Berenfeld B, Hutton M, Davies P. Altered conformation of recombinant frontotemporal dementia-17 mutant tau proteins. Neurosci Lett 1999; 260: 153-156

Johnson GV, Hartigan JA. Tau protein in normal and Alzheimer's disease brain: an update. J Alzheimers Dis 1999; 1: 329-351

Kang J, Lemaire HG, Unterbeck A, Salbaum JM, Masters CL, Grzeschik KH, Multhaup G, Beyreuther K, Muller-Hill B. The precursor of Alzheimer's disease amyloid A4 protein resembles a cell-surface receptor. Nature 1987; 325: 733-6

Kanneganti TD, Ozoren N, Body-Malapel M, Amer A, Park JH, Franchi L, Whitfield J, Barchet W, Colonna M, Vandenabeele P, Bertin J, Coyle A, Grant EP, Akira S, Nunez G. Bacterial RNA and small antiviral compounds activate caspase-1 through cryopyrin/Nalp3. Nature 2006; 440: 233-236

Karran E, Mercken M, De Strooper B. The amyloid cascade hypothesis for Alzheimer's disease: an appraisal for the development of therapeutics. Nat Rev Drug Discov 2011; 10: 698-712

Keren-Shaul H, Spinrad A, Weiner A, Matcovitch-Natan O, Dvir-Szternfeld R, Ulland TK, David E, Baruch K, Lara-Astaiso D, Toth B, Itzkovitz S, Colonna M, Schwartz M, Amit I. A Unique Microglia Type Associated with Restricting Development of Alzheimer's Disease. Cell 2017; 169: 1276-90 e17

Kettenmann H, Hanisch UK, Noda M, Verkhratsky A. Physiology of microglia. Physiol Rev 2011; 91: 461-553

Kitazawa M, Oddo S, Yamasaki TR, Green KN, LaFerla FM. Lipopolysaccharide-induced inflammation exacerbates tau pathology by a cyclin-dependent kinase 5-mediated pathway in a transgenic model of Alzheimer's disease. J Neurosci 2005; 25: 8843-8853

Kusakawa G, Saito T, Onuki R, Ishiguro K, Kishimoto T, Hisanaga S. Calpain-dependent proteolytic cleavage of the p35 cyclin-dependent kinase 5 activator to p25. J Biol Chem 2000; 275: 17166-17172

Lamkanfi M, Dixit VM. Inflammasomes and their roles in health and disease. Annu

Rev Cell Dev Biol 2012; 28: 137-161

Latz E. The inflammasomes: mechanisms of activation and function. Curr Opin Immunol 2010; 22: 28-33

Lawson LJ, Perry VH, Dri P, Gordon S. Heterogeneity in the distribution and morphology of microglia in the normal adult mouse brain. Neuroscience 1990; 39: 151-170

Lee DC, Rizer J, Selenica ML, Reid P, Kraft C, Johnson A, Blair L, Gordon MN, Dickey CA, Morgan D. LPS- induced inflammation exacerbates phospho-tau pathology in rTg4510 mice. J Neuroinflammation 2010; 7: 56

Lew J, Huang QQ, Qi Z, Winkfein RJ, Aebersold R, Hunt T, Wang JH. A brain-specific activator of cyclin-dependent kinase 5. Nature 1994; 371: 423-426

Li Y, Liu L, Barger SW, Griffin WS. Interleukin-1 mediates pathological effects of microglia on tau phosphorylation and on synaptophysin synthesis in cortical neurons through a p38-MAPK pathway. J Neurosci 2003; 23: 1605-1611

Lindwall G, Cole RD. Phosphorylation affects the ability of tau protein to promote microtubule assembly. J Biol Chem 1984; 259: 5301-5305

Liu F, Grundke-Iqbal I, Iqbal K, Gong CX. Contributions of protein phosphatases PP1, PP2A, PP2B and PP5 to the regulation of tau phosphorylation. Eur J Neurosci 2005; 22: 1942-50

Louis JV, Martens E, Borghgraef P, Lambrecht C, Sents W, Longin S, Zwaenepoel K, Pijnenborg R, Landrieu I, Lippens G, Ledermann B, Gotz J, Van Leuven F, Goris J, Janssens V. Mice lacking phosphatase PP2A subunit PR61/B'delta (Ppp2r5d) develop spatially restricted tauopathy by deregulation of CDK5 and GSK3beta. Proc Natl Acad Sci U S A 2011; 108: 6957-62

Lue LF, Rydel R, Brigham EF, Yang LB, Hampel H, Murphy GM, Brachova L, Yan SD, Walker DG, Shen Y, Rogers J. Inflammatory repertoire of Alzheimer's disease

and nondemented elderly microglia in vitro. Glia 2001; 35: 72-79

Luna-Munoz J, Chavez-Macias L, Garcia-Sierra F, Mena R. Earliest stages of tau conformational changes are related to the appearance of a sequence of specific phospho-dependent tau epitopes in Alzheimer's disease. J Alzheimers Dis 2007; 12: 365-75

Mariathasan S, Weiss DS, Newton K, McBride J, O'Rourke K, Roose-Girma M, Lee WP, Weinrauch Y, Monack DM, Dixit VM. Cryopyrin activates the inflammasome in response to toxins and ATP. Nature 2006; 440: 228-232

Martinon F, Petrilli V, Mayor A, Tardivel A, Tschopp J. Gout-associated uric acid crystals activate the NALP3 inflammasome. Nature 2006; 440: 237-241

Martinon F, Tschopp J. NLRs join TLRs as innate sensors of pathogens. Trends Immunol 2005; 26: 447-454

Masumoto J, Taniguchi S, Ayukawa K, Sarvotham H, Kishino T, Niikawa N, Hidaka E, Katsuyama T, Higuchi T, Sagara J. ASC, a novel 22-kDa protein, aggregates during apoptosis of human promyelocytic leukemia HL-60 cells. J Biol Chem 1999; 274: 33835-8

Mattson MP. Pathways towards and away from Alzheimer's disease. Nature 2004; 430: 631-639

Mawuenyega KG, Sigurdson W, Ovod V, Munsell L, Kasten T, Morris JC, Yarasheski KE, Bateman RJ. Decreased clearance of CNS beta-amyloid in Alzheimer's disease. Science 2010; 330: 1774

McGeer PL, McGeer EG. Polymorphisms in inflammatory genes and the risk of Alzheimer disease. Arch Neurol 2001; 58: 1790-1792

Mittelbronn M, Dietz K, Schluesener HJ, Meyermann R. Local distribution of microglia in the normal adult human central nervous system differs by up to one order of magnitude. Acta Neuropathol 2001; 101: 249-255

Morales I, Jimenez JM, Mancilla M, Maccioni RB. Tau oligomers and fibrils induce activation of microglial cells. J Alzheimers Dis 2013; 37: 849-856

Morishima-Kawashima M, Hasegawa M, Takio K, Suzuki M, Yoshida H, Titani K, Ihara Y. Proline-directed and non-proline-directed phosphorylation of PHF-tau. J Biol Chem 1995; 270: 823-829

Netea MG, van de Veerdonk FL, van der Meer JW, Dinarello CA, Joosten LA. Inflammasome-independent regulation of IL-1-family cytokines. Annu Rev Immunol 2015; 33: 49-77

Nicoll JA, Wilkinson D, Holmes C, Steart P, Markham H, Weller RO. Neuropathology of human Alzheimer disease after immunization with amyloid-beta peptide: a case report. Nat Med 2003; 9: 448-452

Nilson AN, English KC, Gerson JE, Barton Whittle T, Nicolas Crain C, Xue J, Sengupta U, Castillo-Carranza DL, Zhang W, Gupta P, Kayed R. Tau Oligomers Associate with Inflammation in the Brain and Retina of Tauopathy Mice and in Neurodegenerative Diseases. J Alzheimers Dis 2017; 55: 1083-1099

Noble W, Hanger DP, Miller CC, Lovestone S. The importance of tau phosphorylation for neurodegenerative diseases. Front Neurol 2013; 4: 83

Noble W, Planel E, Zehr C, Olm V, Meyerson J, Suleman F, Gaynor K, Wang L, LaFrancois J, Feinstein B, Burns M, Krishnamurthy P, Wen Y, Bhat R, Lewis J, Dickson D, Duff K. Inhibition of glycogen synthase kinase-3 by lithium correlates with reduced tauopathy and degeneration in vivo. Proc Natl Acad Sci U S A 2005; 102: 6990-5

Ortega-Gutierrez S, Leung D, Ficarro S, Peters EC, Cravatt BF. Targeted disruption of the PME-1 gene causes loss of demethylated PP2A and perinatal lethality in mice. PLoS One 2008; 3: e2486

Pei JJ, Braak E, Braak H, Grundke-Iqbal I, Iqbal K, Winblad B, Cowburn RF.

Distribution of active glycogen synthase kinase 3beta (GSK-3beta) in brains staged for Alzheimer disease neurofibrillary changes. J Neuropathol Exp Neurol 1999; 58: 1010-1019

Pei JJ, Braak E, Braak H, Grundke-Iqbal I, Iqbal K, Winblad B, Cowburn RF. Localization of active forms of C-jun kinase (JNK) and p38 kinase in Alzheimer's disease brains at different stages of neurofibrillary degeneration. J Alzheimers Dis 2001; 3: 41-48

Pei JJ, Grundke-Iqbal I, Iqbal K, Bogdanovic N, Winblad B, Cowburn RF. Accumulation of cyclin-dependent kinase 5 (cdk5) in neurons with early stages of Alzheimer's disease neurofibrillary degeneration. Brain Res 1998; 797: 267-277

Querfurth HW, LaFerla FM. Alzheimer's disease. N Engl J Med 2010; 362: 329-344

Radde R, Bolmont T, Kaeser SA, Coomaraswamy J, Lindau D, Stoltze L, Calhoun ME, Jaggi F, Wolburg H, Gengler S, Haass C, Ghetti B, Czech C, Holscher C, Mathews PM, Jucker M. Abeta42-driven cerebral amyloidosis in transgenic mice reveals early and robust pathology. EMBO Rep 2006; 7: 940-946

Ramanan VK, Risacher SL, Nho K, Kim S, Shen L, McDonald BC, Yoder KK, Hutchins GD, West JD, Tallman EF, Gao S, Foroud TM, Farlow MR, De Jager PL, Bennett DA, Aisen PS, Petersen RC, Jack CR, Toga AW, Green RC, Jagust WJ, Weiner MW, Saykin AJ, Initiative Alzheimer's Disease Neuroimaging. GWAS of longitudinal amyloid accumulation on 18F-florbetapir PET in Alzheimer's disease implicates microglial activation gene IL1RAP. Brain 2015; 138: 3076-3088

Ransohof RM. A polarizing question: do M1 and M2 microglia exist? Nat Neurosci 2016; 19: 987-991

Sasaguri H, Nilsson P, Hashimoto S, Nagata K, Saito T, De Strooper B, Hardy J, Vassar R, Winblad B, Saido TC. APP mouse models for Alzheimer's disease preclinical studies. EMBO J 2017; 36: 2473-2487

Sastre M, Dewachter I, Landreth GE, Willson TM, Klockgether T, van Leuven F, Heneka MT. Nonsteroidal anti-inflammatory drugs and peroxisome proliferator-activated receptor-gamma agonists modulate immunostimulated processing of amyloid precursor protein through regulation of beta-secretase. J Neurosci 2003; 23: 9796-9804

Scarmeas N, Luchsinger JA, Schupf N, Brickman AM, Cosentino S, Tang MX, Stern Y. Physical activity, diet, and risk of Alzheimer disease. JAMA 2009; 302: 627-637

Schindowski K, Bretteville A, Leroy K, Begard S, Brion JP, Hamdane M, Buee L. Alzheimer's disease-like tau neuropathology leads to memory deficits and loss of functional synapses in a novel mutated tau transgenic mouse without any motor deficits. Am J Pathol 2006; 169: 599-616

Sheedy FJ, Grebe A, Rayner KJ, Kalantari P, Ramkhelawon B, Carpenter SB, Becker CE, Ediriweera HN, Mullick AE, Golenbock DT, Stuart LM, Latz E, Fitzgerald KA, Moore KJ. CD36 coordinates NLRP3 inflammasome activation by facilitating intracellular nucleation of soluble ligands into particulate ligands in sterile inflammation. Nat Immunol 2013; 14: 812-820

Singh TJ, Wang JZ, Novak M, Kontzekova E, Grundke-Iqbal I, Iqbal K. Calcium/calmodulin-dependent protein kinase II phosphorylates tau at Ser-262 but only partially inhibits its binding to microtubules. FEBS Lett 1996; 387: 145-148

Sontag JM, Sontag E. Protein phosphatase 2A dysfunction in Alzheimer's disease. Front Mol Neurosci 2014; 7: 16

Stancu IC, Cremers N, Vanrusselt H, Couturier J, Vanoosthuyse A, Kessels S, Lodder C, Brone B, Huaux F, Octave JN, Terwel D, Dewachter I. Aggregated Tau activates NLRP3-ASC inflammasome exacerbating exogenously seeded and non-exogenously seeded Tau pathology in vivo. Acta Neuropathol 2019; 137: 599-617

Stutz A, Golenbock DT, Latz E. Inflammasomes: too big to miss. J Clin Invest

2009; 119: 3502-3511

Stutz A, Horvath GL, Monks BG, Latz E. ASC speck formation as a readout for inflammasome activation. Methods Mol Biol 2013; 1040: 91-101

Takemura R, Okabe S, Umeyama T, Kanai Y, Cowan NJ, Hirokawa N. Increased microtubule stability and alpha tubulin acetylation in cells transfected with microtubule-associated proteins MAP1B, MAP2 or tau. J Cell Sci 1992; 103: 953-64

Tejera D, Mercan D, Sanchez-Caro JM, Hanan M, Greenberg D, Soreq H, Latz E, Golenbock D, Heneka MT. Systemic inflammation impairs microglial Abeta clearance through NLRP3 inflammasome. EMBO J 2019; 38: e101064

Togo T, Akiyama H, Iseki E, Kondo H, Ikeda K, Kato M, Oda T, Tsuchiya K, Kosaka K. Occurrence of T cells in the brain of Alzheimer's disease and other neurological diseases. J Neuroimmunol 2002; 124: 83-92

Utton MA, Vandecandelaere A, Wagner U, Reynolds CH, Gibb GM, Miller CC, Bayley PM, Anderton BH. Phosphorylation of tau by glycogen synthase kinase 3beta affects the ability of tau to promote microtubule self-assembly. Biochem J 1997; 323 (Pt 3): 741-7

Vande Walle L, Van Opdenbosch N, Jacques P, Fossoul A, Verheugen E, Vogel P, Beyaert R, Elewaut D, Kanneganti TD, van Loo G, Lamkanfi M. Negative regulation of the NLRP3 inflammasome by A20 protects against arthritis. Nature 2014; 512: 69-73

Venegas C, Heneka MT. Danger-associated molecular patterns in Alzheimer's disease. J Leukoc Biol 2017; 101: 87-98

Venegas C, Heneka MT. Inflammasome-mediated innate immunity in Alzheimer's disease. FASEB J 2019; 33: 13075-13084

Venegas C, Kumar S, Franklin BS, Dierkes T, Brinkschulte R, Tejera D, Vieira-

Saecker A, Schwartz S, Santarelli F, Kummer MP, Griep A, Gelpi E, Beilharz M, Riedel D, Golenbock DT, Geyer M, Walter J, Latz E, Heneka MT. Microglia-derived ASC specks cross-seed amyloid-beta in Alzheimer's disease. Nature 2017; 552: 355-361

Walsh DM, Selkoe DJ. Deciphering the molecular basis of memory failure in Alzheimer's disease. Neuron 2004; 44: 181-193

Walsh JG, Muruve DA, Power C. Inflammasomes in the CNS. Nat Rev Neurosci 2014; 15: 84-97

Wang Y, Mandelkow E. Tau in physiology and pathology. Nat Rev Neurosci 2016; 17: 22–35

Weggen S, Eriksen JL, Das P, Sagi SA, Wang R, Pietrzik CU, Findlay KA, Smith TE, Murphy MP, Bulter T, Kang DE, Marquez-Sterling N, Golde TE, Koo EH. A subset of NSAIDs lower amyloidogenic Abeta42 independently of cyclooxygenase activity. Nature 2001; 414: 212-216

Wen H, Ting JP, O'Neill LA. A role for the NLRP3 inflammasome in metabolic diseases--did Warburg miss inflammation? Nat Immunol 2012; 13: 352-7

Whitmer RA, Gunderson EP, Quesenberry CP, Zhou J, Yaffe K. Body mass index in midlife and risk of Alzheimer disease and vascular dementia. Curr Alzheimer Res 2007; 4: 103-109

Woodgett JR. Molecular cloning and expression of glycogen synthase kinase-3/factor A. EMBO J 1990; 9: 2431-2438

Xing Y, Li Z, Chen Y, Stock JB, Jeffrey PD, Shi Y. Structural mechanism of demethylation and inactivation of protein phosphatase 2A. Cell 2008; 133: 154-63

Yamamoto H, Hiragami Y, Murayama M, Ishizuka K, Kawahara M, Takashima A. Phosphorylation of tau at serine 416 by Ca2+/calmodulin-dependent protein kinase II in neuronal soma in brain. J Neurochem 2005; 94: 1438-1447

Yoshiyama Y, Higuchi M, Zhang B, Huang SM, Iwata N, Saido TC, Maeda J, Suhara T, Trojanowski JQ, Lee VM. Synapse loss and microglial activation precede tangles in a P301S tauopathy mouse model. Neuron 2007; 53: 337-351

Zhang B, Gaiteri C, Bodea LG, Wang Z, McElwee J, Podtelezhnikov AA, Zhang C, Xie T, Tran L, Dobrin R, Fluder E, Clurman B, Melquist S, Narayanan M, Suver C, Shah H, Mahajan M, Gillis T, Mysore J, MacDonald ME, Lamb JR, Bennett DA, Molony C, Stone DJ, Gudnason V, Myers AJ, Schadt EE, Neumann H, Zhu J, Emilsson V. Integrated systems approach identifies genetic nodes and networks in late-onset Alzheimer's disease. Cell 2013; 153: 707-720

Zotova E, Bharambe V, Cheaveau M, Morgan W, Holmes C, Harris S, Neal JW, Love S, Nicoll JA, Boche D. Inflammatory components in human Alzheimer's disease and after active amyloid-beta42 immunization. Brain 2013; 136: 2677-2696

9. Acknowledgement

First of all, I would like to gratefully thank Prof. Dr. Michael T. Heneka for giving me the very precious chance to work on this interesting and promising project in his lab. Certainly, this project would never have been finished without his supervision and support.

I am especially thankful to Dr. Ising Christina, for supervising me through my project and thesis. Her support, dedication, advice and ideas have motivated me greatly. I am thankful to Carmen, Stephanie and Ana for providing help on animal models study.

I am very thankful to Sabine, whose expertise in neuron culture experiment was valuable and important for my thesis.

I would like to express appreciation to Dr. McManus and Dr. Dansokho, for scientific advices.

I would like to express gratitude towards Dr. Racz and Angelika for their work in administration and organization.

It gives me pleasure to thank all the members of the laboratory: Dario, Deniz, Dilek, Elena, Francessco, Frederik (Brosseron), Frederik (Eikens), Lea, Marion, Nadia, Paula, Shadi, Tasuya and Tobias, for excellent work environment.

With limited words, it’s inadequate to express my gratitude towards my family and loved ones.